Journal of Medicinal Chemistry

Article

Circumventing Seizure Activity in a Series of G Protein Coupled Receptor 119 (GPR119) Agonists.

James S. Scott, Suzanne S Bowker, Katy J Brocklehurst, Hayley S Brown, David S Clarke, Alison Easter, Anne Ertan, Kristin Goldberg, Julian A Hudson, Stefan Kavanagh, David Laber, Andrew G. Leach, Philip A. MacFaul, Elizabeth A. Martin, Darren McKerrecher, Paul Schofield, Per H Svensson, and Joanne Teague

J. Med. Chem., **Just Accepted Manuscript** • DOI: 10.1021/jm5011012 • Publication Date (Web): 06 Oct 2014

Circumventing Seizure Activity in a Series of G Protein Coupled Receptor 119 (GPR119) Agonists.

James S. Scott,[a] *Suzanne S. Bowker,*[a] *Katy J. Brocklehurst,*[a] *Hayley S. Brown,*[a] *David S. Clarke,*[a] *Alison Easter,*[a] *Anne Ertan,*[c] *Kristin Goldberg,*[a] *Julian A. Hudson,*[a] *Stefan Kavanagh,*[a] *David Laber,*[a] *Andrew G. Leach,*[a] *Philip A. MacFaul,*[a] *Elizabeth A. Martin,*[a] *Darren McKerrecher,*[a] *Paul Schofield,*[a] *Per H. Svensson,*[b] *Joanne Teague.*[a]

Innovative Medicines Unit, AstraZeneca

[a]Mereside, Alderley Park, Macclesfield, Cheshire, SK10 4TG, UK

[b]Pharmaceutical Development, AstraZeneca R&D, S-151 85 Södertälje, Sweden

[c]Current Address: Arrhenius Laboratory, Stockholm University, Department of Materials and Environmental Chemistry, Svante Arrheniusvägen 16C, SE-106 91 Stockholm, Sweden

Abstract

Agonism of GPR119 is viewed as a potential therapeutic approach for the treatment of type II diabetes and other elements of the metabolic syndrome. During progression of a previously disclosed candidate **1** through mice toxicity studies, we observed tonic-clonic convulsions in several mice at high doses. An in vitro hippocampal brain slice assay was used to assess the seizure liability of subsequent compounds leading to the identification of an aryl sulfone as a replacement for the 3-cyano pyridyl group. Subsequent optimization to improve the overall profile, specifically with regard to hERG activity, led to alkyl sulfone **16**. This compound did not cause tonic-clonic convulsions in mice, had a good pharmacokinetic profile and displayed in vivo efficacy in murine models. Importantly, it was shown to be effective in wild-type (WT) but not GPR119 knock-out (KO) animals, consistent with the pharmacology observed being due to agonism of GPR119.

Introduction

G Protein coupled receptor 119 (GPR119) is a class A type receptor that is predominantly expressed in the islets of Langerhans in the pancreas and the enteroendocrine cells of the intestine.[1] Endogenous natural agonists of this receptor, such as oleoylethanolamide (OEA)[2] and *N*-oleoyldopamine (OLDA),[3] have been identified and their biological effects studied. Agonism of GPR119 has been shown to increase the secretion of incretins from L-cells (*e.g.* glucagon-like peptide-1 (GLP-1) and glucose-dependent insulinotropic peptide (GIP),[4] and to stimulate the release of insulin from pancreatic β-cells.[5] Consequently, agonism of GPR119 has been viewed as having considerable potential in the treatment of diabetes.[6,7]

Following an initial disclosure by researchers at Arena that a small molecule agonist was capable of controlling glucose excursions in preclinical animal models,[8] a large volume of patent applications and journal articles have been published disclosing various chemotypes that act as GPR119 agonists. To date, structures of GPR119 agonists have been published by groups including Amgen,[9] Astellas,[10] Boehringer Ingelheim,[11] GlaxoSmithKline,[12] Hoffman-La Roche,[13] Kangwon National University,[14] Pfizer,[15] Merck,[16] Sanwa Kagaku Kenkyusho,[17] Shanghai Institute of Materia Medica[18] and Takeda.[19] Several GPR119 agonists have now been progressed to the clinic (Figure 1) with published clinical data from APD-597 (JNJ-38431055)[8c] (Arena / Johnson & Johnson) demonstrating encouraging increases in GLP-1, GIP and peptide YY levels. However, reductions in glucose excursion and increased insulin secretion were not significant.[20] Clinical data from GSK-1292263 (GlaxoSmithKline) showed a trend towards improvement in insulin sensitivity in healthy subjects, but no reductions in plasma glucose concentrations relative to placebo when tested in type 2 diabetics.[21] An increase in fasting plasma high-density lipoprotein cholesterol was observed, together with a reduction in low-density lipoprotein cholesterol and triglycerides.

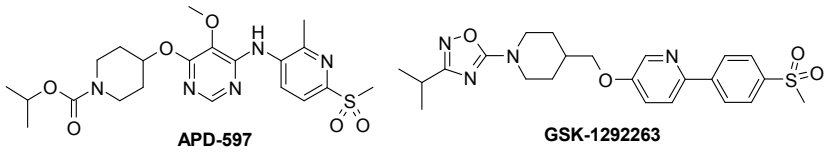

Figure 1. Structures of selected GPR119 agonists with reported clinical data.

Our own efforts to identify novel GPR119 agonists were initially complicated by off-target effects observed in mouse in vivo sudies.[22a] We have subsequently reported on a structurally distinct chemical series that displayed no activity in GPR119 knock-out mice,[22b] our efforts to improve aqueous solubility[22c] and our observations on species differences between mouse and human pharmacology.[22d] We herein report our findings related to the development of compounds from this series and our resulting optimization efforts.

Results & Discussion

Upon progression of a previously disclosed lead compound (**1**)[22b] into mouse toxicity studies, we observed tonic-clonic convulsions in two out of six mice which were subsequently terminated for welfare reasons. The convulsions were observed on the tenth day of the study dosing at 300 mg/kg and exposure levels obtained from one of the premature decedents was 1.0 μM (Cmaxfree) at the time of termination on day 10. This alerted us to the fact that our compounds potentially carried a seizure liability, a fact we felt was unacceptable for a high quality compound intended for the treatment of diabetes. We therefore sought to identify a method for identifying this liability without recourse to large scale toxicity studies and identified an in vitro hippocampal brain slice model as a potential way to assess compounds.[23] This involved recording the electrophysiology of evoked synaptic activity of a mouse hippocampal brain slice using extracellular electrodes positioned in the CA1 cell body layer in the presence of compound. Increases in population spikes, quantified as areas above and below the 0 mV baseline, were associated with an increased risk of seizure activity. Results from the screening of an initial set of four compounds are shown in Figure 2. Compound **1**, which had observations of tonic-clonic convulsions in the mouse toxicity study, showed changes in peak shape and quantifiable increases in peak area upon increasing dose, characteristic of a seizureogenic compound and was classified as positive in this assay. Likewise

compounds **2** and **3** were flagged as positive, seizureogenic compounds in this assay. In contrast, compound **4** showed no discernable activity and was classified as unlikely to be seizureogenic (negative) in this assay. The common structural motif for compounds **1-3** was the 3-cyano pyridyl moiety with compounds **3** and **4** representing a molecular matched pair of compounds where the 3-cyano pyridyl had been replaced with a 2-fluoro arylsulfone.

Figure 2. Results from brain-slice assay showing the profile for compound **1**, the mean dose response for compound **1** and the structures of compounds tested (**1-4**). Statistical significance is denoted as: * $p < 0.05$, ** $p < 0.01$, *** $p < 0.001$.

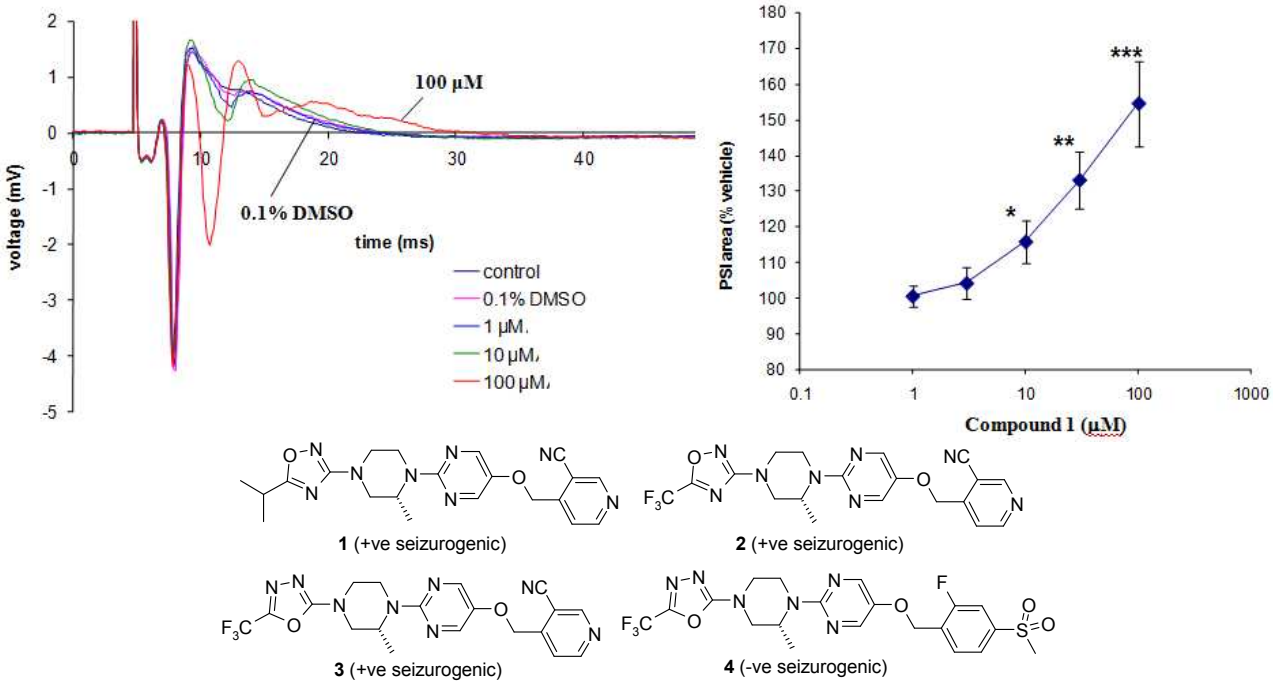

We concluded that a pragmatic way to mimimise the seizureogenic risk would be to avoid compounds with the 3-cyano pyridyl motif and seek to re-optimise this portion of the molecule and screen promising candidates in the in vitro brain slice model. To this end, we embarked on an optimisation campaign with the syntheses of the compounds described below.

Synthesis.

For variation of the left hand side of the molecule (Scheme 1), routes were developed starting from the previously described[22b] Boc protected piperazine pyrimidinol **25**. Alkylation under basic conditions afforded the benzyl ethers **26**. Removal of the Boc group with hydrochloric acid gave the piperazines **27** which could be converted to the 3-(trifluoromethyl)oxetane carbamates **20** – **22** through treatment with the corresponding perfluorophenyl carbonates. Alternatively, treatment of **27** with cyanogen bromide gave the versatile intermediate cyanamides **28**. Treatment with the appropriate amidoximes in the presence of zinc chloride, followed by ring closure under acidic conditions afforded the 1,2,4-oxadiazoles with 3-substitution of either CF_3 (**15**, **16**) or iPr (**23**, **24**). Alternatively, the cyanamides **28** could be treated with sodium azide to form the tetrazoles **29**. Treatment with trifluoroacetic anhydride following by heating effected a conversion to the 1,3,4-oxadiazoles **4** and **11**.

Scheme 1[a]

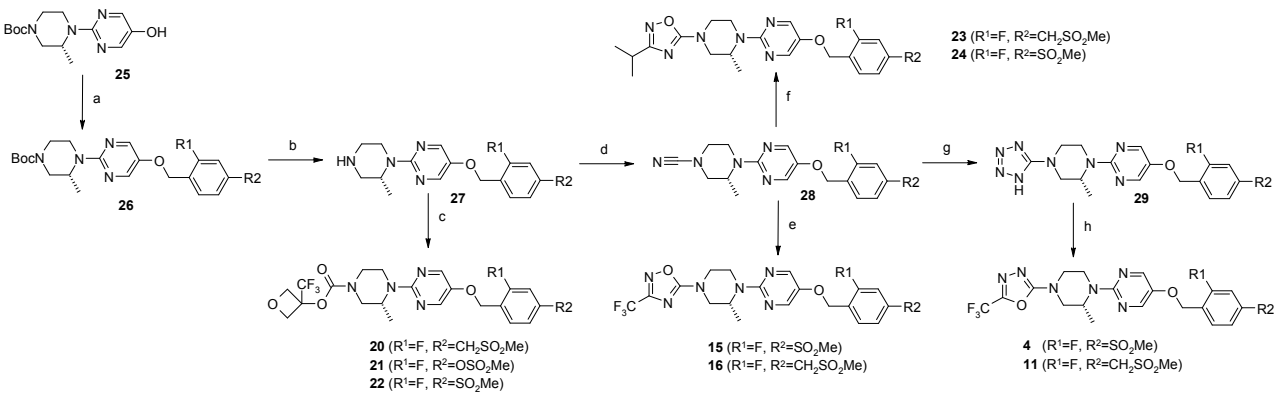

[a] Reagents and Conditions: (a) $ArCH_2Br$, Cs_2CO_3, CH_3CN, 20 °C, 3 d, 29-81%; (b) HCl, CH_2Cl_2, 25 °C, 16 h 76-100%; (c) (3-(CF_3)oxetan-3-yl)$OCOOC_6F_5$, NEt_3, $CHCl_3$, 25 °C, 18 h, 67-94%; (d) CNBr, $NaHCO_3$, CH_2Cl_2/H_2O, 25 °C, 2 h, 87-89%; (e) (i) $CF_3C(=NOH)NH_2$, $ZnCl_2$, EtOAc/THF, 20 °C, 4 h; (ii) conc. HCl, EtOH, 100 °C, 18 h, 34-55%; (f) (i) $^iPrC(=NOH)NH_2$, $ZnCl_2$, EtOAc/THF, 20 °C, 4 h; (ii) conc. HCl, EtOH, 100 °C, 16 h, 19-85%; (g) NaN_3, NEt_3.HCl, toluene, 80 °C, 3 d, 87%-100%; (h) $(CF_3CO)_2O$, $(^iPr)_2NEt$, chlorobenzene, 130 °C, 2 h, 61-88%.

For exploration of the right hand side (Scheme 2), complementary routes were established that allowed construction of the heterocycles prior to alkylation. Boc protected piperazine pyrimidinol **25** was treated with acid to give the piperazine **30** and then with cyanogen bromide to give cyanamide **31**. Both the 1,3,4-oxadazole **32** and the 1,2,4-oxadazole **33** could be constructed using analogous chemistry to that described in Scheme 1, notably without requirement for protection of the phenol. Subsequent alkylations with the requisite benzyl bromides (**7** – **9**), mesylates (**10-14**, **18**) or chlorides (**19**) afforded the final compounds. Alkylation with 2-cyano-4-bromo-benzylbromide afforded intermediate **34**. The aryl bromide could be transformed into either a sulfone or cyano group to afford compounds **5** and **6** respectively.

Scheme 2[a]

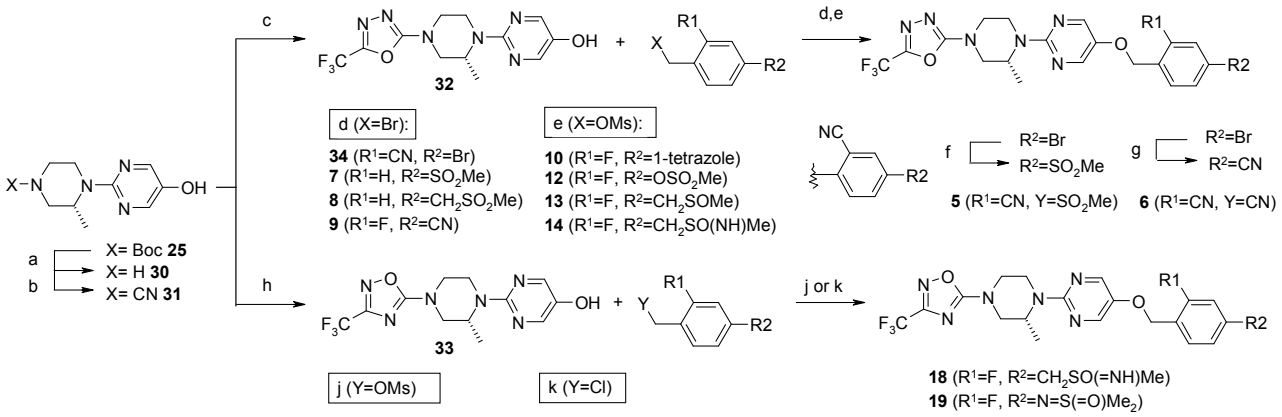

[a] Reagents and Conditions: (a) HCl, 1,4-dioxane/CH_2Cl_2, 20 ^oC, 90 min 98%; (b) CNBr, $NaHCO_3$, CH_2Cl_2/H_2O, 25 ^oC, 1 h, 59%; (c) (i) NaN_3, NEt_3.HCl, toluene, 80 ^oC, 18 h, 87%-100%; (ii) $(CF_3CO)_2O$, $(^iPr)_2NEt$, toluene, 250 ^oC, 4 d, 19%; (d) $ArCH_2Br$, K_2CO_3, DMF, 25 ^oC, 16 h, 47-89%; (e) $ArCH_2OMs$, K_2CO_3, DMF, 25 ^oC, 16 h, 12-32%; (f) CF_3SO_3Cu, $(MeNHCH_2)_2$, DMSO, CH_3SO_2Na, 120 ^oC, 2 h, 61%; (g) $Zn(CN)_2$, $Pd(dba)_2$, Xantphos, DMF, 130 ^oC, 2 h, μW, 78%; (h) $CF_3C(=NOH)NH_2$, $ZnCl_2$, EtOAc/THF, 20 ^oC, 24 h; (ii) conc. HCl, EtOH, 110 ^oC, 18 h, 58%; (j) (i) $ArCH_2OMs$, K_2CO_3, CH_3CN, 75 ^oC, 4 h; (ii) K_2CO_3, MeOH, 50 ^oC, 2 h; 19%; (k) $ArCH_2Cl$, K_2CO_3, DMF, 100 ^oC, 35 h, 16%.

Other examples, such as sulfoxide **17**, were synthesised by functional group manipulation of the benzyl substituent whilst attached to the core (Scheme 3). Previously described bromide **35**[22b] was lithiated and quenched with DMF to form the aldehyde **36** then reduced using sodium borohydride to the primary alcohol **37**. Formation of the mesylate allowed introduction of a thiomethyl group under ambient conditions to give sulfide **38**. Mono-oxidation to the sulfoxide **39** was achieved using Oxone® at 0 °C and a short reaction time of 15 minutes. The Boc group was then removed under acidic conditions and the piperazine converted to cyanamide **40** in good yield. Subsequent treatment with trifluoromethyl amidoxime in the presence of zinc chloride and heating under acid conditions afforded the sulfoxide **17** in low yield.

Scheme 3[a]

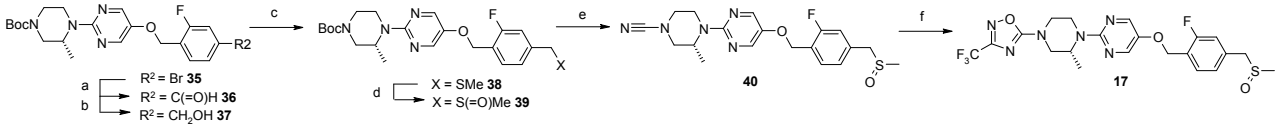

[a] Reagents and Conditions: (a) ^{n}BuLi, THF, -78 °C, DMF, 1 h, 83%; (b) $NaBH_4$, EtOH, rt, 3 h, 91%; (c) (i) MsCl, CH_2Cl_2, rt, 18 h; (ii) MeSNa, DMF, rt, 18 h, 42%; (d) Oxone®, MeOH/MeCN/H_2O, 0 °C 15 min, 100%; (e) (i) TFA, CH_2Cl_2, 20 °C, 3 h; (ii) CNBr, $NaHCO_3$, CH_2Cl_2/H_2O, 0 °C, rt, 2 h, 88%; (f) (i) $CF_3C(=NOH)NH_2$, $ZnCl_2$, EtOAc/THF, rt, 2 h; (ii) conc. HCl, EtOH, reflux, 16 h, 16%.

Medicinal Chemistry

The results of our strategy of replacing the 3-cyanopyridyl group in **3** is shown in Table 1. Replacement with a 3-fluoro sulfone group gave compound **4** which had broadly similar potency when tested on HEK cells transfected to overexpress human GPR119 receptors, albeit with reduced intrinsic activity (IA). In the analogous mouse GPR119 HEK system, an improvement in potency was observed (EC_{50} = 144 nM, IA 93%).[24] In line with our previous observations, this compound was much less soluble and somewhat surprisingly showed increased inhibition of the hERG ion channel tail current using a plate-based planar patch clamp system (IonWorks™; IC_{50} = 6.9 μM).[25] The 3-cyano analogue **5** lost potency against the

mouse receptor and showed no benefit in terms of hERG inhibition. The corresponding di-cyano compound **6**, where the sulfone was replaced with a cyano group, showed enhanced potency in human and mouse however the solubility remained low and this compound suffered from high hERG inhibition (IC_{50} = 3.6 μM). The des-fluoro sulfone **7** had reduced potency relative to the 3-fluoro molecular matched pair **4** in line with previously reported SAR. Extending the sulfone out by insertion of a methylene group gave compound **8** which had a similar profile to compound **7** in terms of potency, lipophilicity and solubility but showed no detectable inhibition of the hERG ion channel.[26] Compound **9**, the cyano analogue of sulfone **4**, showed similar potency but higher lipophilicity ($logD_{7.4}$ = 3.8) and poor aqueous solubility.[27] The *N*-tetrazole **10** was more potent in both human and mouse but showed no improvement in terms of solubility or hERG. The methylene extended sulfone **11** was of comparable potency to the aryl sulfone **4** and again showed no discernable inhibition of the hERG ion channel (c.f. matched pair **7** and **8**). This observation prompted further exploration around this area with replacement of the methylene with an oxygen atom leading to aryl mesylate **12**. This compound showed increased potency, albeit at the expense of increased lipophilicity,[28] and some weak hERG activity (IC_{50} = 17 μM). The sulfoxide **13** was less potent, but less lipophilic and showed no hERG inhibition. Notably the aqueous solubility improved significantly relative to the sulfone although, perhaps unsurprisingly, metabolic instability increased as measured in rat hepatocytes (Cl_{int} = 53 μl/min/10^6 cells for **13**, Cl_{int} = 9 μl/min/10^6 cells for **11**). The corresponding sulfoximine **14** was less lipophilic and showed a further increase in aqueous solubility and no hERG inhibition. Human potency was reduced, broadly in line with the lipophilicity reduction, however, in mouse a loss of intrinsic activity at the receptor precluded further progression of this compound.

Table 1. Variation in the 1,3,4-oxadiazole series.

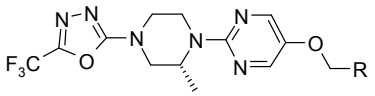

Cpd	R	human GPR119 EC_{50} (μM)[a]	human GPR119 IA (%)[b]	mouse GPR119 EC_{50} (μM)[a]	mouse GPR119 IA (%)[b]	$logD_{7.4}$[c]	Solubility (μM)[d]	hERG IC_{50} (μM)[e]
3	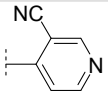	0.028 (0.027-0.029)	220 (209-230)	0.436 (0.383-0.497)	94 (90-99)	2.7	120	18
4	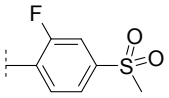	0.021 (0.019-0.023)	121 (114-127)	0.144 (0.128-0.163)	93 (88-89)	3.0	1.4	6.9
5	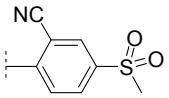	0.055 (0.049-0.061)	182 (171-192)	1.975 (1.291-3.022)	252 (143-362)	2.6	9.3	6.4
6	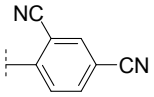	0.010 (0.008-0.011)	166 (155-176)	0.072 (0.056-0.091)	84 (72-96)	2.8	1.9	3.6
7	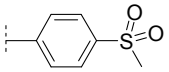	0.133 (0.110-0.160)	119 (110-127)	0.297 (0.229-0.386)	71 (68-74)	2.8	2.4	9.4
8	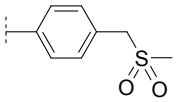	0.150 (0.131-0.172)	89 (86-92)	0.319 (0.269-0.377)	95 (90-100)	2.6	2.3	>30
9	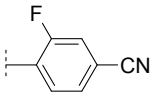	0.015 (0.014-0.017)	156 (141-171)	0.216 (0.154-0.303)	90 (80-101)	3.8	<0.5	11
10	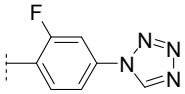	0.007 (0.006-0.007)	170 (149-191)	0.058 (0.050-0.067)	91 (85-97)	3.6	0.8	5.7
11	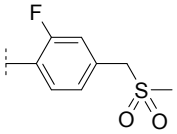	0.027 (0.025-0.029)	100 (95-105)	0.249 (0.227-0.274)	100 (95-106)	2.9	3.8	>30

12	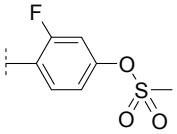	0.004 (0.003-0.004)	156 (143-169)	0.042 (0.038-0.046)	82 (75-88)	3.7	2.3	17
13	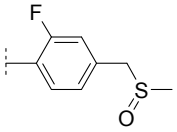	0.058 (0.051-0.066)	139 (132-137)	0.976 (0.861-1.107)	85 (79-92)	2.6	84	>30
14	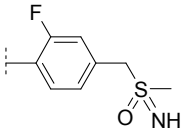	0.158 (0.141-0.178)	101 (90-113)	>5	47 (43-52)	2.1	370	>30

[a]EC_{50} data are the geometric mean of at least three independent measurements, with 68% confidence limits in parentheses as calculated from SEM. [b]Intrinsic activity expressed as the percent effect compared to that of the control, 50 μM oleoylethanolamide, defined as 100%. [c]Distribution coefficient between 1-octonol and aqueous phosphate buffer at pH 7.4. [d]Solubility of compounds in aqueous phospahte buffer at pH7.4 after 24 hours at 25 ^{o}C. [e]Inhibition of the hERG ion channel using an electrophysiology (IonWorks^{TM}) patch clamp system.

Based on previous investigations in this area, we believed that the 1,2,4-oxadiazole isomers should be more lipophilic than their 1,3,4-isomers and this potentially offered an opportunity to increase potency (Table 2).[29] Sulfone **15** was indeed more potent against human and mouse than **4**, but remained potent against hERG. By contrast, the methylene extended sulfone **16** again showed no discernable hERG activity and had improved potency against the human and mouse isoforms relative to **11**. The SAR/SPR observed in this sub-series showed similar trends to those described in Table 1; the sulfoxide **17** having similar potency and improved solubility and the sulfoximine **18** showing a reduction in potency, broadly in line with lipophilicity, and a large increase in solubility and little or no hERG activity. An isomeric sulfoximine **19** was less active, despite being much more lipophilic, and had poor solubility although it too remained devoid of hERG activity.

Table 2. Variation in the 1,2,4-oxadiazole series.

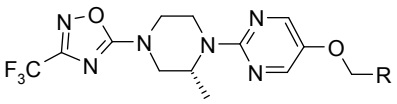

Cpd	R	human GPR119 EC_{50} (μM)[a]	human GPR119 IA (%)[b]	mouse GPR119 EC_{50} (μM)[a]	mouse GPR119 IA (%)[b]	$logD_{7.4}$[c]	Solubility (μM)[d]	hERG IC_{50} (μM)[e]
15	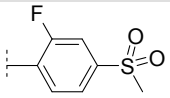	0.004 (0.003-0.004)	89 (85-93)	0.030 (0.023-0.039)	78 (71-85)	3.7	<1.4	3.6
16	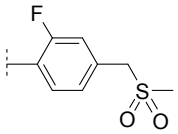	0.011 (0.010-0.012)	84 (79-89)	0.068 (0.059-0.079)	71 (65-76)	3.6	1.8	>30
17	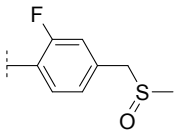	0.008 (0.007-0.010)	108 (101-114)	0.106 (0.094-0.120)	58 (57-59)	3.4	49	28
18	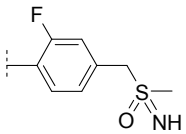	0.091 (0.082-0.102)	57 (53-61)	0.492 (0.333-0.726)	62 (45-78)	2.8	140	>30
19	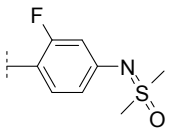	1.102 (0.943-1.287)	27 (26-29)	0.389 (0.351-0.430)	27 (19-34)	3.4	2.6	>30

[a]EC_{50} data are the geometric mean of at least three independent measurements, with 68% confidence limits in parentheses as calculated from SEM with the exception of the human value for **18** which is n=2. [b]Intrinsic activity expressed as the percent effect compared to that of the control, 50 μM oleoylethanolamide, defined as 100%. [c]Distribution coefficient between 1-octonol and aqueous phosphate buffer at pH 7.4. [d]Solubility of compounds in aqueous phospahte buffer at pH7.4 after 24 hours at 25 °C. [e]Inhibition of the hERG ion channel using an electrophysiology (IonWorks™) patch clamp system.

A subsequent round of optimization investigated optimal combinations of groups around the central scaffold (Table 3). Replacement of the oxadiazole with a 2-trifluoromethyloxetane carbamate identified previously,[22c] gave compound **20** with similar potency to **16** but reduced lipophilicity. Unfortunately, this did not translate to improved aqueous solubility. Aryl mesylate **21** was more potent, however the lipophilicity increase associated with the switch from carbon to oxygen further eroded the aqueous solubility of this compound. It is noteworthy that both compounds showed no hERG activity in contrast to the direct linked sulfone equivalent **22**, which had a similar overall profile but did show inhibition of the hERG ion channel (IC_{50} = 11 μM). Replacing the trifluroromethyl group of **16** with an isopropyl substituent resulted in **23** which was less potent, in line with lower lipophilicity. No inhibition of hERG was observed whereas the molecular matched pair **24**, with the direct linked sulfone, did show activity (IC_{50} = 7.4 μM), again emphasizing the lack of hERG activity in the CH_2SO_2Me sub-series.

Table 3. Combination compounds.

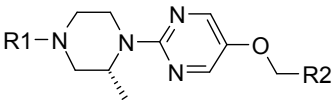

Cpd	R1	R2	human GPR119 EC_{50} (μM)[a]	human GPR119 IA (%)[b]	mouse GPR119 EC_{50} (μM)[a]	mouse GPR119 IA (%)[b]	$logD_{7.4}$[c]	Solubility (μM)[d]	hERG IC_{50} (μM)[e]
20	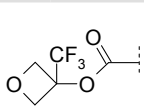	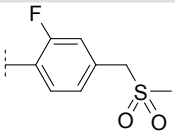	0.020 (0.018-0.022)	91 (88-95)	0.140 (0.123-0.159)	108 (99-117)	2.9	2.5	>30
21	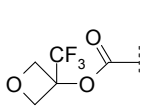	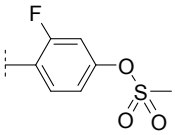	0.004 (0.004-0.005)	141 (133-150)	0.028 (0.024-0.031)	98 (89-107)	3.7	<0.6	>30

22	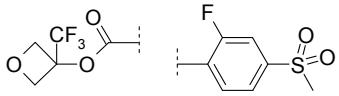	0.012 (0.012-0.013)	99 (93-105)	0.080 (0.073-0.087)	100 (94-106)	3.0	<1.8	11
23	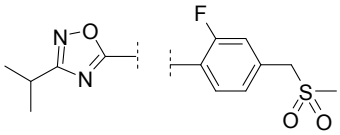	0.018 (0.015-0.022)	93 (75-111)	0.160 (0.120-0.214)	66 (57-75)	3.1	2.4	>30
24	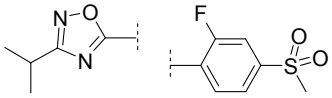	0.006 (0.005-0.007)	101 (97-105)	0.060 (0.050-0.072)	83 (78-87)	3.4	1.0	7.4

[a]EC_{50} data are the geometric mean of at least three independent measurements, with 68% confidence limits in parentheses as calculated from SEM. [b]Intrinsic activity expressed as the percent effect compared to that of the control, 50 μM oleoylethanolamide, defined as 100%. [c]Distribution coefficient between 1-octonol and aqueous phosphate buffer at pH 7.4. [d]Solubility of compounds in aqueous phospahte buffer at pH7.4 after 24 hours at 25 ^{o}C. [e]Inhibition of the hERG ion channel using an electrophysiology (IonWorks^{TM}) patch clamp system.

A plot of the human potency (pEC_{50} sized by % intrinsic activity) against measured $logD_{7.4}$ is shown in Figure 3A with selected compounds from the manuscript labeled.[30] A well defined leading edge of potency/lipophilicicity is apparent from this dataset. Figure 3B shows the potency increase associated with switching from matched pairs in the 1,3,4-oxadiazole isomers (Table 1) to the 1,2,4-oxadiazole isomers (Table 2) and Figure 3C shows that this is primarily driven by a consistent increase in lipophilicity associated with this change.

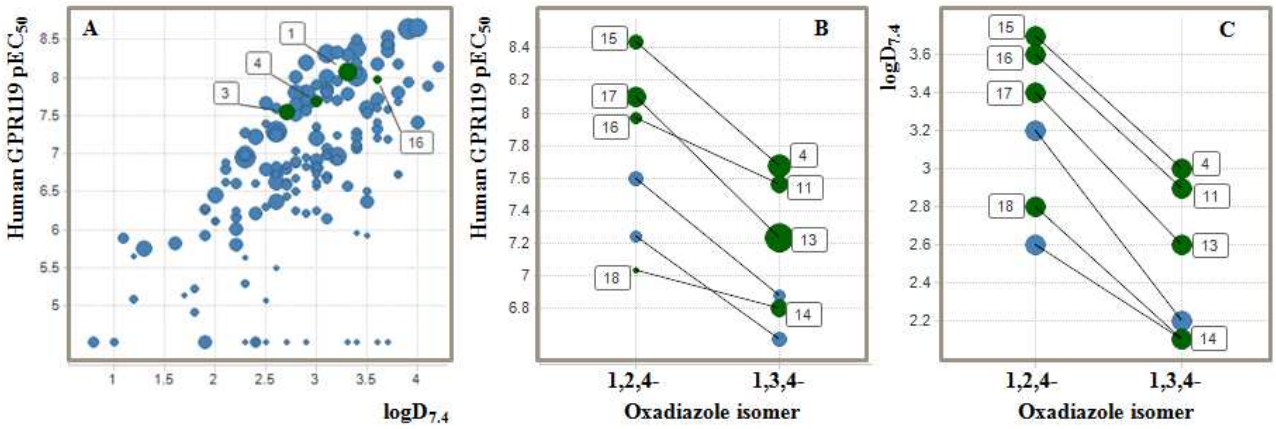

Figure 3. A) Plot of human GPR119 pEC_{50} sized by intrinsic activity (%) against measured $logD_{7.4}$; B) Plot of human GPR119 pEC_{50} for 1,2,4- and 1,3,4-oxadiazole matched pairs; Plot of measured $logD_{7.4}$ for 1,2,4- and 1,3,4-oxadiazole matched pairs. Selected compounds are annotated with their corresponding manuscript numbers.

A selected set of compounds (**11**, **16**, **20**) were selected for profiling in the in vitro brain slice model. All of these compounds showed no discernable change in peak shape upon increasing concentration and were therefore classified as low for seizureogenic risk. The data for compound **16** is shown in Figure 4 and, in contrast to Figure 2, shows no increases in population spikes or peak area upon increasing compound concentration. On the overall balance of properties, compound **16** was selected for further evaluation in a 12 day mouse toxicity study specifically designed and powered (n=8) to assess seizure liability. In contrast to the tonic-clonic convulsions observed with **1**, no evidence for seizures in any of the animals was observed during the course of this study with mean free exposures of **16** achieved during the study of 0.7 µM Cmaxfree. This data, taken together with the lack of signal from the brain slice assay and adequate safety margins achieved with this study, provided confidence to continue to progress this compound.

Figure 4. Results from brain-slice assay showing the profile & mean dose response for compound **16** with aminophylline (4-AP) used as positive control

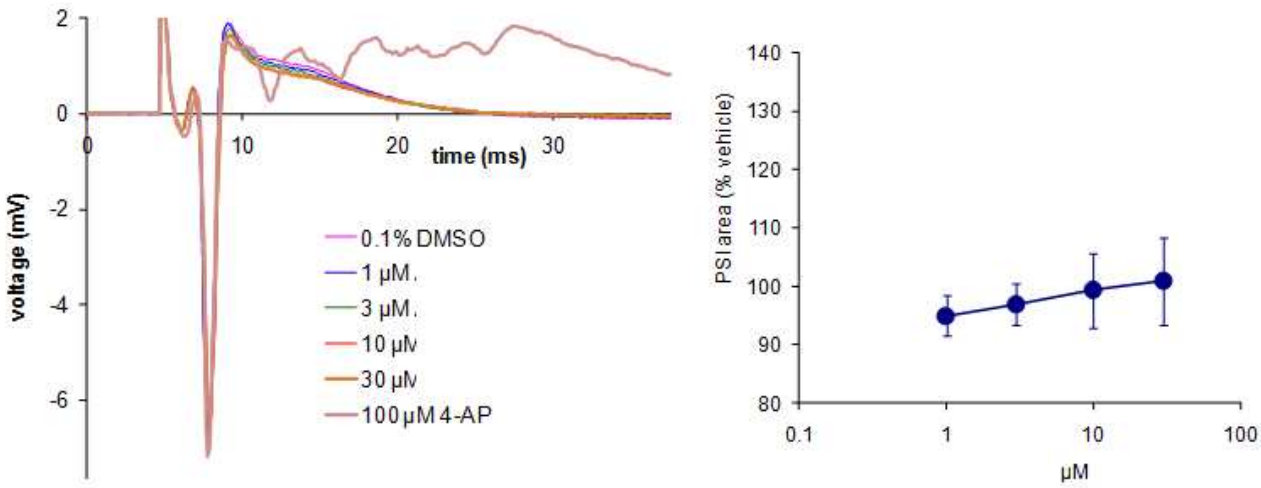

Further profiling of **16** showed no inhibition (IC_{50} values > 10 μM) of five cytochrome P450 enzymes (CYP1A2, CYP2C9, CYP2C19, CYP2D6 and CYP3A4) in a high throughput fluorescence assay. Plasma protein binding showed less than three fold variation across species (mouse 1.2% free; rat 1.5% free; dog 1.6% free; human 0.6% free). The aqueous solubility at pH 7.4 as measured at 25 ^{o}C on crystalline material was low (1.8 μM), however, it was shown to be higher (38 μM) in biologically relevant media at 37 ^{o}C.[31] Permeability, as measured in an in vitro Caco-2 assay, was high with no evidence of efflux (apical to basolateral Papp $10x10^{-6}$ cm/s at a compound concentration of 10 μM; efflux ratio 0.6). Compound **16** showed no photolytic instability or hydrolytic instability across the pH range 1-8, although some degredation was noted at pH 10.[32] The secondary pharmacology profile was clean against a panel of 100 targets with the only hit being weak activity against the epidermal growth factor receptor (IC_{50} = 2.1 μM). The compound showed no discernable activity (IC_{50} > 30 μM) against a selection of ion channels (hERG, NaV1.5, Ito, CaV1.2) and only very weak activity against the cardiac K^+ channel I_{Ks} (IC_{50} = 27 μM) which was not considered as an issue. Compound **16** was non-mutagenic in a two-strain Ames test and negative in a mouse lymphoma assay.

The small molecule crystal structure of **16** shows that the compound adopts a structure broadly similar to that of the equivalent aryl sulfones: a layer of adjacent molecules (Figure 5a) is arranged into stacks. A

key difference is that the introduction of the extra methylene group has caused the molecules shape to be stepped at one end and this in turn translates into a stepped shape of the layers that the molecules are arranged in (Figure 5b). The layers are held together by interactions between the polarized CHs of the pyrimidine interacting with one of the sulfone oxygens while the sulfone methyl interacts with a pyrimidine nitrogen. All of these weak donor and acceptor features are also present in the structure of the aryl sulfone but interact in different combinations.[22b] By contrast to the flatter aryl sulfone, the molecules do not arrange themselves in a head to head fashion that allows the sulfone of one molecule to interact with that of an adjacent one. As shown in Figure 5c, the layers are held together by ladders of interactions involving the sulfones with the benzylic methylene and the sulfone methyl CHs both acting as weak donors and interacting with one of the sulfone oxygens. Finally, the molecules do not stack perfectly on top of one another (Figure 5d), this offset has been observed previously in this series[22b] when the methyl group is added to the piperazine. Although the aqueous solubility of **16** remains low, these differerences potentially contribute to improvements seen in respect to the original sulphone lead in this series.[22b]

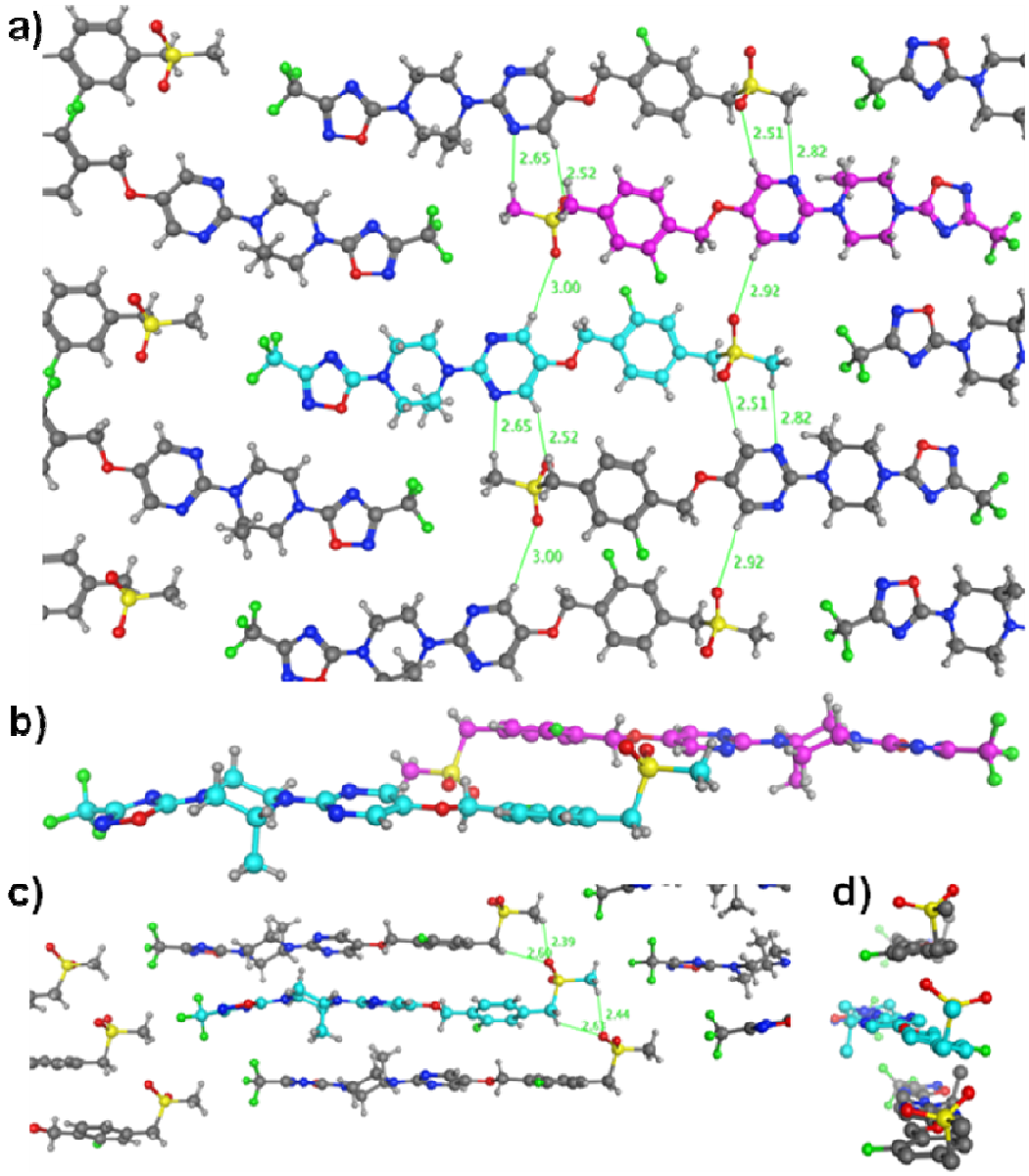

Figure 5. Four views of the crystal structure of compound **16**. a) shows the plane of adjacent molecules from above. b) shows the stepped arrangement of adjacent molecules in the plane shown in a). c) shows how the molecules stack on top of one another viewed from the side of the molecules and d) shows how the molecules stack viewed from the end of the molecules. Distances shown are in Å.

Pharmacokinetics

Plasma pharmacokinetic parameters (IV and PO) for compound **16** were determined in C57BL6 mice (male), Han Wistar rats (male) and beagle dogs (male and female). The compound was administered

orally (PO) as a suspension in aqueous 0.1% (w/v) Pluronic F127 and intravenously (IV) as a solution in 5% DMSO:95% hydroxylpropyl β-cyclodextrin, at relevant pharmacological doses (2-5 mg/kg) as shown in Table 4. The compound was characterized by low clearance (Clp), especially in dog, and moderate volume of distribution (V_{ss}), consistent across the three species. The in vivo clearance results were in good accordance with the in vitro predictions based on hepatocyte data (Cl_{int} 7 and 10 µl/min/10^6 cells, respectively) and plasma protein binding free levels (1.2% and 1.5%, respectively) for mouse and rat. There was no discernible turnover in either dog or human hepatocytes (Cl_{int} <2 µl/min/10^6 cells) which fitted well with the low clearance observed in dog and gave confidence that the compound would be low clearance in humans. Bioavailability (F) and fraction absorbed (F_{abs}) were high for all three species which was somewhat surprising given the low aqueous solubility, and may reflect the improved solubility observed in biologically relevant media (vide supra).

Table 4. Pharmacokinetic parameters for compound **16**[a]

Species	Clp (mL/min/kg)	Vss (L/kg)	PO half-life (h)	IV half-life (h)	F_{abs}	F (%)
Mouse	9.8	5.1	6.9	6.3	0.8	76
Rat	11	5.2	6.7	6.1	1.0	85
Dog	1.6	3.3	30	26	1.0	98

[a]Compounds were dosed intravenously at either 2 mg/kg (rat and dog) or 3 mg/kg (mouse) in 5% DMSO:95% hydroxylpropyl β-cyclodextrin and orally as either 5 mg/kg (mouse and rat) or 3.4 mg/kg (dog) using a 0.1% HMPC / tween suspension (mouse and rat) or 0.1% Pluronic F127 suspension (dog), respectively at volumes of 4 mL/kg (mouse and rat) and 2 mL/kg (dog).

In order to address concerns that exposure at higher doses would be limited by solubility, oral dose escalation studies were carried out as shown in Table 5. These results showed significant increases in

exposure of compound upon increasing compound dose, both in terms of maximum plasma concentration observed (C_{max}) and area under the curve (AUC), alleviating these concerns and providing confidence that compound **16** could be evaluated in pre-clinical toxicity studies.

Table 5. Exposure from rising dose pharmacokinetic studies for compound **16**

Species	Dose[a]	C_{max}[b]	AUC[c]	Species	Dose[a]	C_{max}[b]	AUC[c]
Rat	4.5	0.8	10	Dog	5	1.5	20
Rat	7.1	1.1	11	Dog	50	3.2	42
Rat	12	3.4	33	Dog	98	5.3	78
Rat	19	7.5	106	Mouse	5.7	2.5	26
Rat	100	8.0	123	Mouse	11	3.3	35
Rat	154	13.7	247	Mouse	31	11.8	151
				Mouse	57	29.0	456

[a]Dose is in mg/kg from a suspension of 0.1% Pluronic F127 in fed animals. [b]C_{max} is measured in μM. [c]AUC = $AUC_{0\text{-}24hr}$ (μM.h) in all studies. All data is the mean of the results from two animals; in the case of the dog, one male and one female.

In vivo Efficacy

Compound **16** was profiled in vivo for its ability to control the glucose excursion in a mouse (C57BL6/JAX) oral glucose tolerance test (OGTT).[33] As shown in Figure 6a, **16** enhances glucose disposal in a dose-dependant (1.5 - 15 mg/kg) manner with a minimum efficacious dose of 1.5 mg/kg. In a separate study, the ability of compound **16** to increase the levels of total GLP-1 in systemic circulation

was investigated. Total GLP-1 levels were measured 30 minutes after an oral dose of the compound and showed a dose-dependent increase with significant elevation at doses of 5 mg/kg (Figure 6b).

Figure 6. Oral administration of compound **16** dose dependently enhances glucose disposal and increases GLP-1 secretion in lean mice.[a]

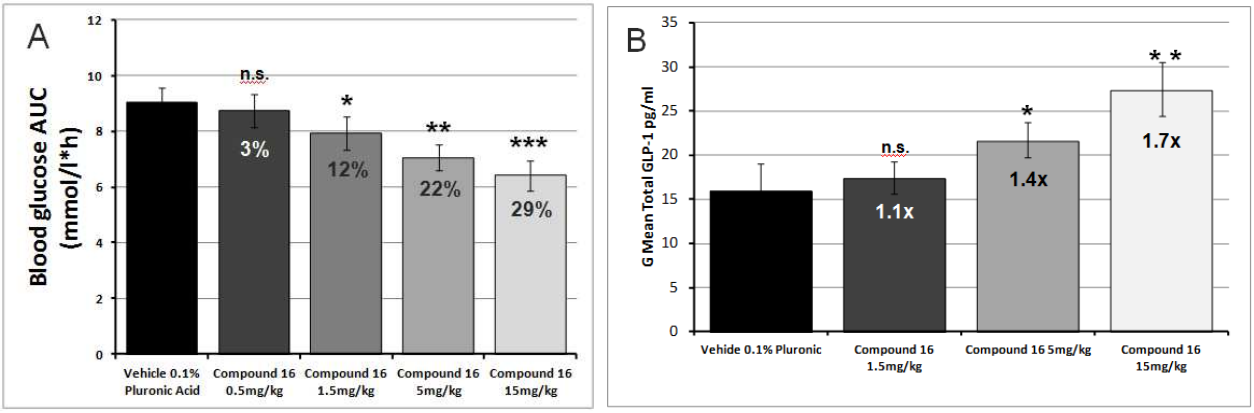

[a]A) Dose-effect of cpd **16** on blood glucose in male C57BL6/j mice. Group sizes (n) - Vehicle control (24); Cpd **16** - 0.5mg/kg (18), 1.5mg/kg (17), 5mg/kg (18) & 15mg/kg (18). Cpd **16** was administered 30 minutes prior to an oral glucose load of 2 g/kg and glucose blood levels were monitored out to 90 minutes Variables & covariates (Time 0 & Start) have not been logged. Percentage reduction in blood glucose AUC calculated relative to window between Vehicle control and zero. One-sided Student t test for a decreasing effect using pooled inter-animal variability (all groups included in the analysis). B) Dose-effect of cpd 16 on blood total GLP-1 in male C57BL6/j mice. Group sizes (n) - Vehicle control (19); Cpd 16 - 1.5mg/kg (20), 5mg/kg (20) & 15mg/kg (20). Cpd **16** was administered to fasted animals 30 minutes prior to terminal blood sampling for total GLP-1 measurements & Fold increase in GLP-1 calculated relative to vehicle control. Variables have been logged & all groups included in an ANCOVA analysis (Start as a covariate) using One-sided Student t test for an increasing effect. Statistical significance for glucose and GLP effects is denoted as: * $p < 0.05$, ** $p < 0.01$, *** $p < 0.001$.

Confirmation that agonism of GPR119 was responsible for the observed pharmacology was established by assessing compound **16** in an OGTT with both wild-type (WT) and GPR119 knock-out (KO) mice. At a dose of 15 mg/kg of **16**, the wild-type animals showed clear evidence of enhanced glucose disposal (22%) whereas in the knock-out mice, no significant effect was observed (Figure 7).

Figure 7. Compound **16** enhances glucose disposal (OGTT) in WT but not GPR119 KO mice.[a]

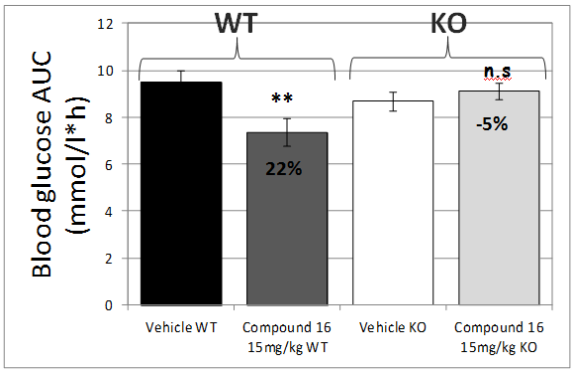

[a] Cpd **16** blood glucose reduction showing GPR119 dependency in male wild-type (WT) and knock-out (KO) mice. Group sizes (n) - Vehicle control (WT=16, KO=16); Cpd **16** - 15mg/kg (WT=10, KO=10). Cpd **16** was administered 30 minutes prior to an oral glucose load of 2 g/kg and glucose blood levels were monitored out to 90 minutes Variables & covariates (Time 0 & Start) have not been logged. Percentage reduction in blood glucose AUC calculated relative to window between Vehicle control and zero. One-sided Student t test for a decreasing effect using pooled inter-animal variability (all groups included in the analysis but results of the other test groups have been excluded for simplicity). Statistical significance is denoted as: * $p < 0.05$, ** $p < 0.01$, *** $p < 0.001$.

With evidence that compound **16** was displaying robust, on-target efficacy at 5 mg/kg, we examined the pharmocology of compound **42** in an OGTT in combination with the dipeptidyl peptidase-4 (DPPIV) inhibitor sitagliptin at a dose of 0.3 mg/kg. DPPIV inhibitors achieve their efficacy through preventing the inactivation of GLP-1 thus prolonging the effect of this incretin hormone.[34] The combination of a

GPR119 agonist with a DPPIV inhibitor is therefore attractive as a therapeutic paradigm as it should both elevate and prolong the levels of GLP-1. In an OGTT experiment, the combination of **16** with sitagliptin showed a statistically significant benefit over each monotherapy (Figure 8).

Figure 8. Combination of compound **16** and sitagliptin shows benefit in glucose disposal over monotherapy.[a]

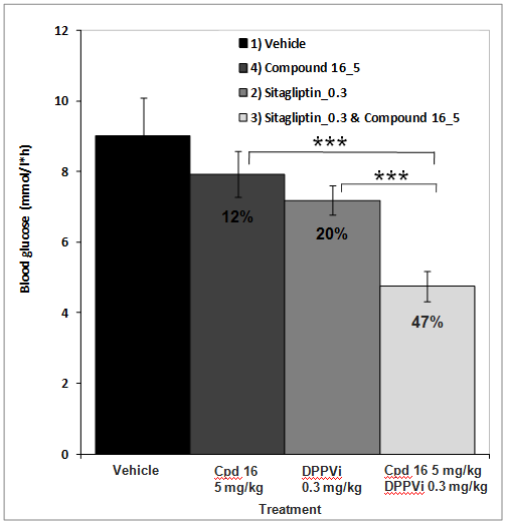

[a] Glucose-lowering effect of GPR119 agonist (cpd **16**) co-administered with DPPIV inhibitor (sitagliptin) in an Oral Glucose Tolerance Test (OGTT) in male C57BL6/Jax mice. Group sizes (n) - Vehicle control (8), Cpd **16** - 5mg/kg (11), sitagliptin 0.3 mg/kg (11) & combination (11). Control or test compound was administered 30 minutes prior to a glucose load of 2 g/kg and glucose levels monitored out to 90 minutes. Glucose response AUC's (variable baseline) for test groups were compared to vehicle control by ANCOVA analysis (Time 0 covariate). Glucose AUC in the combination therapy group was compared to each monotherapy AUC. Statistical significance is denoted as: * $p < 0.05$, ** $p < 0.01$, *** $p < 0.001$.

On the basis of the attractive profile and pharmacokinetics together with the in vivo results showing clear, on target efficacy at low doses and an improved safety profile relative to **1**, compound **16** was selected for further development, the results of which will be reported in due course.

Conclusion

Upon observing tonic-clonic convulsions in toxicity studies in mice at high doses with a previously disclosed candidate **1**, we established an in vitro brain slice assay to assess the seizure liability of subsequent compounds. This led to the identification of an aryl sulfone **4** as a replacement for the 3-cyano pyridyl group that avoided this liability. Subsequent optimisation to improve the overall profile, specifically with regard to hERG activity, led to alkyl sulfone **16**. This compound did not cause tonic-clonic convulsions in mice, had a good pharmacokinetic profile and displayed in vivo efficacy in murine models. Importantly, similar efficacy was not seen in GPR119 knock-out mice confirming that the pharmacology observed was through agonism of GPR119.

Experimental Section

General Procedures. All solvents and chemicals used were reagent grade. Flash column chromatography was carried out using prepacked silica cartridges (from 4 g up to 330 g) from Redisep, Biotage, or Crawford and eluted using an Isco Companion system. ^{1}H NMR were recorded on a Bruker Avance DPX400 (400 MHz) and were determined in $CDCl_3$ or DMSO-d_6. ^{13}C NMR spectra were recorded at 101 or 175 MHz. Chemical shifts are reported in ppm relative to tetramethylsilane (TMS) (0.00 ppm) or solvent peaks as the internal reference and coupling constant (J) values are reported in Hertz (Hz). Splitting patterns are indicated as follows: s, singlet; d, doublet; t, triplet; m, multiplet. Merck precoated thin layer chromatography (TLC) plates (silica gel 60 F_{254}, 0.25 mm, art. 5715) were used for TLC analysis. The purity of compounds submitted for screening was >95% as determined by UV analysis of liquid chromatography-mass spectroscopy (LC-MS) chromatograms at 254 nM and substantiated using the TAC (Total Absorption Chromatogram). Further support for the purity statement was provided using the MS TIC (Total Ion Current) trace in ESI +ve and –ve ion modes, HRMS and NMR analysis. Solutions were dried over anhydrous magnesium sulfate, and solvent was removed by rotary evaporation under reduced pressure. Melting points were determined on a Mettler FP62 automatic melting point

apparatus and are uncorrected. The synthesis of selected examples are described below, for complete details on all intermediates and final compounds please refer to the supplementary material. All experimental activities involving animals were carried out in accordance with AstraZeneca animal welfare protocols which are consistent with The American Chemical Society Publications rules and ethical guidelines.

5-{[2-fluoro-4-(methylsulfonyl)benzyl]oxy}-2-{(2*R*)-2-methyl-4-[5-(trifluoromethyl)-1,3,4-oxadiazol-2-yl]piperazin-1-yl}pyrimidine (4). To a stirred suspension of (*R*)-5-(2-fluoro-4-(methylsulfonyl)benzyloxy)-2-(2-methyl-4-(1H-tetrazol-5-yl)piperazin-1-yl)pyrimidine (3.68 g, 8.21 mmol) and *N*-ethyldiisopropylamine (4.3 mL, 24.6 mmol) in chlorobenzene (75 mL) under an atmosphere of nitrogen was added trifluoroacetic anhydride (2.3 mL, 16.4 mmol) at 0 °C. The mixture was heated at 130 °C for 16 hours, cooled to ambient temperature, partitioned between ethyl acetate (425 mL) and water (175 mL), the ethyl acetate layer washed with saturated sodium hydrogen carbonate solution, brine, dried ($MgSO_4$) and evaporated in vacuo to a residue which was chromatographed on silica with 50% ethyl acetate in isohexane as eluant, then on neutral alumina with 25% ethyl acetate in isohexane as eluant to give a solid which was crystallised from ethyl acetate / isohexane to give (*R*)-2-(4-(5-(2-fluoro-4-(methylsulfonyl)benzyloxy)pyrimidin-2-yl)-3-methylpiperazin-1-yl)-5-(trifluoromethyl)-1,3,4-oxadiazole (2.60 g, 61%). m.p. 145 – 146 °C; ^{1}H NMR (400 MHz, $CDCl_3$) 1.25 (3H, d, *J* = 6.7 Hz), 3.08 (3H, s), 3.22 - 3.38 (2H, m), 3.46 (1H, dd, *J* = 4.0, 12.9 Hz), 3.89 (1H, dt, *J* = 1.7, 12.9 Hz), 4.02 - 4.15 (1H, m), 4.50 - 4.63 (1H, m), 4.95 - 5.03 (1H, m), 5.17 (2H, s), 7.70 (1H, dd, *J* = 1.5, 8.9 Hz), 7.73 - 7.84 (2H, m), 8.18 (2H, s); ^{13}C NMR (176 MHz, DMSO) 13.7, 37.3, 43.1, 45.3, 45.6, 49.6, 65.0, 114.3 (d, *J* = 24.4 Hz), 116.1 (q, *J* = 269 Hz), 123.1, 129.5 (d, *J* = 14.7 Hz), 131.2 (d, *J* = 3.8 Hz), 142.5 (d, *J* = 6.7 Hz), 145.0, 146.4, 147.4 (q, *J* = 43.0 Hz), 156.7, 159.6 (d, *J* = 251 Hz), 165.2; HRMS (EI) for $C_{20}H_{21}O_4N_6SF_4$ (MH^+); calcd, 517.1276; found, 517.1274.

5-(methylsulfonyl)-2-{[(2-{(2R)-2-methyl-4-[5-(trifluoromethyl)-1,3,4-oxadiazol-2-yl]piperazin-1-yl}pyrimidin-5-yl)oxy]methyl}benzonitrile (5). To a stirred solution of (*R*)-5-bromo-2-((2-(2-methyl-4-(5-(trifluoromethyl)-1,3,4-oxadiazol-2-yl)piperazin-1-yl)pyrimidin-5-yloxy)methyl)benzonitrile (230 mg, 0.44 mmol), (trifluoromethylsulfonyloxy)copper (18.65 mg, 0.09 mmol) and *N*,*N*-dimethylethane-1,2-diamine (15.47 mg, 0.18 mmol) in DMSO (2.9 mL) at ambient temperature under an atmosphere of nitrogen was added sodium methanesulfinate (263 mg, 2.19 mmol). The mixture was heated at 120 °C for 2 hours, cooled to ambient temperature, partitioned between ethyl acetate (60 mL) and water (45 mL), washed with water (1 x 20 mL), brine (2 x 20 mL), dried ($MgSO_4$) and evaporated *in vacuo* to a residue which was chromatographed on silica with 50% - 100% ethyl acetate in *iso*hexane as eluant to give (*R*)-2-((2-(2-methyl-4-(5-(trifluoromethyl)-1,3,4-oxadiazol-2-yl)piperazin-1-yl)pyrimidin-5-yloxy)methyl)-5-(methylsulfonyl)benzonitrile (140 mg, 61%). m.p. 65-66 °C; ^{1}H NMR (400 MHz, $CDCl_3$) 1.19 (3H, d, *J* = 6.8 Hz), 3.05 (3H, s), 3.17 - 3.32 (2H, m), 3.47 (1H, dd, *J* = 4.0, 12.9 Hz), 3.91 (1H, dt, *J* = 1.7, 12.9 Hz), 4.04 - 4.17 (1H, m), 4.53 -4.64 (1H, m), 4.96 - 5.06 (1H, m), 5.31 (2H, s), 7.95 (1H, d, *J* = 8.1 Hz), 8.20 - 8.25 (3H, m), 8.30 (1H, d, *J* = 1.8 Hz); ^{13}C NMR (176 MHz, DMSO) 13.7, 37.3, 43.0, 45.3, 45.6, 49.6, 69.0, 112.2, 115.8, 116.1 (q, *J* = 267 Hz), 130.2, 131.5, 132.0, 141.4, 145.0, 146.5, 147.4 (q, *J* = 43.2 Hz), 156.8, 165.2; HRMS (EI) for $C_{21}H_{21}O_4N_7SF_3$ (MH^+); calcd, 524.1322; found, 524.1324.

4-{[(2-{(2*R*)-2-methyl-4-[5-(trifluoromethyl)-1,3,4-oxadiazol-2-yl]piperazin-1-yl}pyrimidin-5-yl)oxy]methyl}benzene-1,3-dicarbonitrile (6). To a mixture of (*R*)-5-bromo-2-((2-(2-methyl-4-(5-(trifluoromethyl)-1,3,4-oxadiazol-2-yl)piperazin-1-yl)pyrimidin-5-yloxy)methyl)benzonitrile (230 mg, 0.44 mmol), zinc cyanide (41.2 mg, 0.35 mmol), tris(dibenzylideneacetone)dipalladium(0) (16.1 mg, 0.02 mmol) and 4,5-bis(diphenylphosphino)-9,9-dimethylxanthene (20.3 mg, 0.04 mmol) in a microwave vial under an atmosphere of nitrogen was added degassed DMF (1.83 mL). The stirred mixture was heated at 130 °C in a Biotage Initiator Microwave oven for 2 hours, cooled to ambient temperature, poured onto water (28 mL) and extracted with ethyl acetate (3 x 25 mL). The combined ethyl acetate extracts washed with brine, dried ($MgSO_4$) and evaporated *in vacuo* to a residue which was chromatographed on silica with 30% - 50% ethyl acetate in *iso*hexane as eluant to give (*R*)-4-((2-(2-methyl-4-(5-(trifluoromethyl)-

1,3,4-oxadiazol-2-yl)piperazin-1-yl)pyrimidin-5-yloxy)methyl)isophthalonitrile (160 mg, 78%). m.p. 123 – 124 °C; ^{1}H NMR (400 MHz, $CDCl_3$) 1.26 (3H, d, *J* = 6.7 Hz), 3.25 - 3.40 (2H, m), 3.40 (1H, dd, *J* = 4.0, 12.9 Hz), 3.91 (1H, dt, *J* = 1.7, 12.9 Hz), 4.04 - 4.13 (1H, m), 4.53 - 4.64 (1H, m), 4.97 - 5.06 (1H, m), 5.27 (2H, s), 7.87 (1H, d, *J* = 8.1 Hz), 7.90 (1H, dd, *J* = 1.5, 8.1 Hz), 7.95 (1H, d, *J* = 1.5 Hz), 8.22 (2H, s); ^{13}C NMR (176 MHz, DMSO) 13.7, 37.3, 45.3, 45.6, 49.6, 69.1, 112.2, 112.4, 115.4, 116.4 (q, *J* = 266 Hz), 130.1, 136.9, 137.1, 144.7, 145.0, 146.6, 147.4 (q, *J* = 43.0 Hz), 156.8, 165.2; HRMS (EI) for $C_{21}H_{18}O_2N_8F_4$ (MH^+); calcd, 471.1499; found, 471.1498.

5-{[4-(methylsulfonyl)benzyl]oxy}-2-{(2R)-2-methyl-4-[5-(trifluoromethyl)-1,3,4-oxadiazol-2-yl]piperazin-1-yl}pyrimidine (7). To a stirred suspension of (*R*)-2-(2-methyl-4-(5-(trifluoromethyl)-1,3,4-oxadiazol-2-yl)piperazin-1-yl)pyrimidin-5-ol (260 mg, 0.79 mmol) and 1-(bromomethyl)-4-(methylsulfonyl)benzene (196 mg, 0.79 mmol) in DMF (2.45 mL) at ambient temperature was added potassium carbonate (163 mg, 1.18 mmol). The mixture was stirred at ambient temperature for 16 hours, the mixture partitioned between water (40 mL) and ethyl acetate (50 mL), the ethyl acetate layer washed with brine, dried ($MgSO_4$) and evaporated *in vacuo* to a residue which was chromatographed on silica with 50% ethyl acetate in *iso*hexane as eluant to give a solid which was crystallised from ethyl acetate / *iso*hexane to give (*R*)-2-(3-methyl-4-(5-(4-(methylsulfonyl)benzyloxy)pyrimidin-2-yl)piperazin-1-yl)-5-(trifluoromethyl)-1,3,4-oxadiazole (300 mg, 76%). m.p. 152 – 153 °C; ^{1}H NMR (400 MHz, $CDCl_3$) 1.26 (3H, d, *J* = 6.7 Hz), 3.07 (3H, s), 3.25 - 3.39 (2H, m), 3.47 (1H, dd, *J* = 4.0, 12.9 Hz), 3.90 (1H, dt, *J* = 1.7, 12.9 Hz), 4.04 - 4.15 (1H, m), 4.52 - 4.62 (1H, m), 4.96 - 5.04 (1H, m), 5.14 (2H, s), 7.63 (2H, d, *J* = 7.3 Hz), 7.99 (2H, d, *J* = 7.3 Hz), 8.16 (2H, s); ^{13}C NMR (176 MHz, DMSO) 13.6, 37.2, 43.4, 45.3, 45.6, 49.6, 70.0, 116.1 (q, *J* = 269 Hz), 127.1, 128.1, 140.3, 142.5, 145.1, 146.2, 147.3 (q *J* = 43.0 Hz), 156.6, 165.2; HRMS (EI) for $C_{20}H_{22}O_4N_6SF_3$ (MH^+); calcd, 499.1370; found, 499.1368.

5-{[2-fluoro-4-(methylsulfonyl)benzyl]oxy}-2-{(2*R*)-2-methyl-4-[3-(trifluoromethyl)-1,2,4-oxadiazol-5-yl]piperazin-1-yl}pyrimidine (15). Zinc chloride (1M in diethyl ether) (0.987 mL, 0.99 mmol) was added to (*R*)-4-(5-(2-fluoro-4-(methylsulfonyl)benzyloxy)pyrimidin-2-yl)-3-

methylpiperazine-1-carbonitrile (400 mg, 0.99 mmol) and 2,2,2-trifluoro-*N*'-hydroxyacetimidamide (171 mg, 1.33 mmol) in ethyl acetate (7 mL) and THF (6 mL) over a period of 2 minutes under nitrogen. The resulting solution was stirred at 20 °C for 3 days. The solvents were removed in vacuo and the residue triturated with diethyl ether to give a white solid. This was dissolved in ethanol (25 mL) then concentrated HCl (2.0 mL) was added over a period of 2 minutes under nitrogen. The resulting solution was stirred at 70 °C for 18 hours. It was cooled to room temperature, concentrated in vacuo and azeotroped once with toluene to give a pale yellow solid. The material was taken up in CH_2Cl_2, concentrated in vacuo and adsorbed onto silica. The crude product was purified by flash silica chromatography, elution gradient 0 to 100% EtOAc in CH_2Cl_2. Pure fractions were evaporated to dryness to afford (*R)*-5-(4-(5-(2-fluoro-4-(methylsulfonyl)benzyloxy)pyrimidin-2-yl)-3-methylpiperazin-1-yl)-3-(trifluoromethyl)-1,2,4-oxadiazole (278 mg, 55%) as a white solid. m.p. 118 – 119 °C; ^{1}H NMR (400 MHz, DMSO) 1.13 (3H, d, *J* = 6.7 Hz), 3.21 - 3.56 (6H, m), 3.83 - 3.94 (1H, m), 3.98 - 4.08 (1H, m), 4.36 - 4.46 (1H, m), 4.80 - 4.94 (1H, m), 5.27 (2H, s), 7.77 - 7.88 (3H, m), 8.34 (2H, s); ^{13}C NMR (176 MHz, DMSO) 13.6, 37.3, 43.2, 45.4, 45.8, 49.8, 65.0, 114.3 (d, *J* = 24.4 Hz), 118.1 (q, *J* = 273 Hz), 123.1 (d, *J* = 3.2 Hz), 129.5 (d, *J* = 14.7 Hz), 131.3 (d, *J* = 3.7 Hz), 142.5 (d, *J* = 6.6 Hz), 145.1, 146.4, 156.7, 159.6 (d, *J* = 252 Hz), 160.6 (q, *J* = 24.4 Hz), 172.1; HRMS (EI) for $C_{20}H_{21}O_4N_6SF_4$ (MH^+); calcd, 517.1276; found, 517.1274.

5-({2-fluoro-4-[(methylsulfonyl)methyl]benzyl}oxy)-2-{(2*R*)-2-methyl-4-[3-(trifluoromethyl)-1,2,4-oxadiazol-5-yl]piperazin-1-yl}pyrimidine (16). Zinc chloride (1M in diethyl ether) (0.715 mL, 0.72 mmol) was added to (*R*)-4-(5-(2-fluoro-4-(methylsulfonylmethyl)benzyloxy)pyrimidin-2-yl)-3-methylpiperazine-1-carbonitrile (300 mg, 0.72 mmol) and 2,2,2-trifluoro-*N*'-hydroxyacetimidamide (124 mg, 0.97 mmol) in ethyl acetate (4.5 mL) and THF (4.0 mL) over a period of 2 minutes under nitrogen. The resulting solution was stirred at 20 °C for 4 hours. The solvents were removed in vacuo, leaving a white foam that was triturated with diethyl ether (10 mL) This was dissolved in ethanol (15 mL) and fuming HCl (2 mL) was added. The resulting suspension was stirred at 100 °C for 18 hours. It was cooled to room temperature and the solvent removed in vacuo. The residue was azeotroped once with toluene to

leave a yellow gum (846 mg). It was taken up in CH_2Cl_2 and adsorbed onto silica. The crude product was purified by flash silica chromatography, elution gradient 0 to 50% EtOAc in CH_2Cl_2. Pure fractions were evaporated to dryness to afford (*R*)-5-(4-(5-(2-fluoro-4-(methylsulfonylmethyl)benzyloxy)pyrimidin-2-yl)-3-methylpiperazin-1-yl)-3-(trifluoromethyl)-1,2,4-oxadiazole (129 mg, 34%) as a white solid. m.p. 124 – 125 °C; ^{1}H NMR (400 MHz, $CDCl_3$) 1.23 (3H, d, *J* = 6.7 Hz), 2.82 (3H, s), 3.27 – 3.38 (2H, m), 3.50 (1H, dd, *J* = 4.0, 13.1 Hz), 4.00 (1H, dt, *J* = 1.6, 13.1 Hz), 4.13 – 4.21 (1H, m), 4.24 (2H, s), 4.50 - 4.61 (1H, m), 4.95 - 5.04 (1H, m), 5.11 (2H, s), 7.18 - 7.28 (3H, m), 7.54 (1H, t, *J* = 7.6 Hz), 8.17 (2H, s); ^{13}C NMR (176 MHz, $CDCl_3$) 13.6, 37.3, 45.4, 45.7, 49.7, 58.6, 65.3, 117.7, 118.1 (q, *J* = 268 Hz), 123.6, 127.0, 130.8, 131.9, 145.3, 146.3, 156.6, 159.9 (d, *J* = 246 Hz), 160.6 (q, *J* = 12.3 Hz), 172.1; HRMS (EI) for $C_{21}H_{23}O_4N_6SF_4$ (MH^+); calcd, 531.1432; found, 531.1429.

5-({2-fluoro-4-[(methylsulfinyl)methyl]benzyl}oxy)-2-{(2R)-2-methyl-4-[3-(trifluoromethyl)-1,2,4-oxadiazol-5-yl]piperazin-1-yl}pyrimidine (17). To a stirred solution of (3*R*)-4-(5-(2-fluoro-4-(methylsulfinylmethyl)benzyloxy)pyrimidin-2-yl)-3-methylpiperazine-1-carbonitrile (290 mg, 0.72 mmol) and 2,2,2-trifluoro-*N*'-hydroxyacetimidamide (124 mg, 0.97 mmol) in a mixture of ethyl acetate (4.31 mL) and tetrahydrofuran (2.87 mL) under an atmosphere of nitrogen was added a 1.0M solution of zinc chloride (1.581 mL, 1.58 mmol) in diethyl ether at ambient temperature over 10 minutes. The mixture was stirred at ambient temperature for 2 hours, the solvents evaporated *in vacuo* to a residue which was taken up in ethanol (4.31 mL) and treated with hydrochloric acid (3.59 mL, 7.19 mmol) and the mixture heated under reflux for 16 hours. The mixture was cooled to ambient temperature, the ethanol evaporated *in vacuo* to a residue which was partitioned between ethyl acetate (75 mL) and saturated sodium hydrogen carbonate solution (25 mL), the ethyl acetate layer washed with brine, dried ($MgSO_4$) and evaporated *in vacuo* to a residue which was chromatographed on silica with ethyl acetate as eluant to give a solid which was crystallised from ethyl acetate / *iso*hexane to give 5-((3*R*)-4-(5-(2-fluoro-4-(methylsulfinylmethyl)benzyloxy)pyrimidin-2-yl)-3-methylpiperazin-1-yl)-3-(trifluoromethyl)-1,2,4-oxadiazole (61 mg, 16%). m.p. 128 – 129 °C; ^{1}H NMR (400 MHz, $CDCl_3$) 1.24 (3H, d, *J* = 6.7 Hz), 2.51 (3H, s), 3.27 - 3.39 (2H, m), 3.51 (1H, dd, *J* = 4.0, 13.1 Hz), 3.96 (2H, s), 4.01 (1H, dt, *J* = 1.6, 13.1 Hz),

4.13 - 4.21 (1H, m), 4.50 - 4.61 (1H, m), 4.95 - 5.04 (1H, m), 5.11 (2H, s), 7.09 (1H, dd, *J* = 1.5, 10.2 Hz), 7.04 (1H, dd, *J* = 1.4, 7.8 Hz), 7.51 (1H, t, *J* = 7.6 Hz), 8.18 (2H, s); HRMS (EI) for $C_{21}H_{23}O_3N_6SF_4$ (MH^+); calcd, 515.1483; found, 515.1478.

(*R*)-3-(trifluoromethyl)oxetan-3-yl 4-(5-(2-fluoro-4-(methylsulfonyl)benzyloxy)pyrimidin-2-yl)-3-methylpiperazine-1-carboxylate (22). Triethylamine (3.3 mL, 23.6 mmol) was added to perfluorophenyl 3-(trifluoromethyl)oxetan-3-yl carbonate (1.46 g, 3.93 mmol) and (*R*)-5-(2-fluoro-4-(methylsulfonyl)benzyloxy)-2-(2-methylpiperazin-1-yl)pyrimidine (1.50 g, 3.93 mmol) in chloroform (15 mL) at 20 °C. The reaction was stirred at 20 °C for 2 hours. The reaction mixture was diluted with CH_2Cl_2 (100 mL), and washed with water (50 mL). The organic layer was dried over $MgSO_4$, filtered and evaporated to afford crude material. The crude product was purified by flash silica chromatography, elution gradient 0 to 80% EtOAc in isohexane. Pure fractions were evaporated to dryness to afford a clear gum which when triturated with diethyl ether gave (*R*)-3-(trifluoromethyl)oxetan-3-yl 4-(5-(2-fluoro-4-(methylsulfonyl)benzyloxy)pyrimidin-2-yl)-3-methylpiperazine-1-carboxylate (1.450 g, 67%) as a white solid. m.p. 119 – 120 °C; ^{1}H NMR (400 MHz, $CDCl_3$) 1.17 (3H, d, *J* = 7 Hz), 3.08 (3H, s), 2.88 – 3.35 (3H, m), 3.83 – 4.20 (2H, m), 4.41 (1H, t, *J* = 13 Hz), 4.78 – 4.92 (3H, m), 4.96 (1H, d, *J* = 9 Hz), 5.05 (1H, d, *J* = 8 Hz), 5.16 (2H, s), 7.69 (1H, dd, *J* = 9, 2 Hz), 7.72 – 7.83 (2H, m), 8.16 (2H, s); ^{13}C NMR (176 MHz, DMSO) 12.9, 13.5, 38.0, 38.2, 43.1, 43.2, 43.9, 46.0, 46.2, 47.3, 48.4, 65.0, 74.0, 75.6 (m), 114.28 (d, *J* = 24.5 Hz), 123.1 (d, *J* = 1.8 Hz), 123.7 (q, *J* = 286 Hz), 129.5(d, *J* = 14.7 Hz), 131.21 (d, *J* = 3.7 Hz), 142.5(d, *J* = 6.7 Hz), 145.0, 146.4, 151.6, 151.8, 156.8, 159.57 (d, *J* = 252 Hz); HRMS (EI) for $C_{22}H_{24}F_4N_4O_6S$ (MH^+); calcd, 549.1425; found, 549.1425.

5-{[2-fluoro-4-(methylsulfonyl)benzyl]oxy}-2-{(2R)-2-methyl-4-[3-(propan-2-yl)-1,2,4-oxadiazol-5-yl]piperazin-1-yl}pyrimidine (24). To a stirred solution of (*R*)-4-(5-(2-fluoro-4-(methylsulfonyl)benzyloxy)pyrimidin-2-yl)-3-methylpiperazine-1-carbonitrile (300mg, 0.74 mmol) and *N'*-hydroxyisobutyrimidamide (102 mg, 1.00 mmol) in a mixture of ethyl acetate (6.0 mL) and tetrahydrofuran (4.0 mL) under an atmosphere of nitrogen was added a 1.0M solution of zinc chloride

(1.628 mL, 1.63 mmol) in diethyl ether at ambient temperature over 10 minutes. The mixture was stirred at ambient temperature for 2 hours then the solvents were evaporated *in vacuo* to a residue which was taken up in ethanol (6.00 mL) and treated with hydrochloric acid (0.617 mL, 7.40 mmol) and the mixture heated under reflux for 16 hours. The mixture was cooled to ambient temperature, the ethanol evaporated *in vacuo* to a residue which was partitioned between ethyl acetate (25 mL) and saturated sodium hydrogen carbonate solution (25 mL), the ethyl acetate layer washed with brine, dried ($MgSO_4$) and evaporated *in vacuo* to a residue which was chromatographed on silica with 50 % ethyl acetate in *iso*hexane as eluant to give a solid which was crystallised from ethyl acetate / heptane to give (*R*)-5-(4-(5-(2-fluoro-4-(methylsulfonyl)benzyloxy)pyrimidin-2-yl)-3-methylpiperazin-1-yl)-3-isopropyl-1,2,4-oxadiazole (70.0 mg, 19%). m.p. 151 – 153 °C; ^{1}H NMR (400 MHz, $CDCl_3$) 1.22 (3H, d, *J* = 6.7 Hz), 1.30 (6H, d, *J* = 6.9 Hz), 2.92 (1H, hept, *J* = 6.9 Hz), 3.08 (3H, s), 3.17 - 3.34 (2H, m), 3.41 (1H, dd, *J* = 4.0, 13.0 Hz), 3.95 (1H, dt, *J* = 1.7, 13.0 Hz), 4.06 - 4.20 (1H, m), 4.41 - 4.56 (1H,), 4.83 - 5.03 (1H, m), 5.17 (2H, s), 7.70 (1H, dd, *J* = 1.5, 8.9 Hz), 7.72 - 7.84 (2H, m), 8.17 (2H, s); ^{13}C NMR (176 MHz, DMSO) 13.7, 20.2, 26.2, 37.5, 43.2, 45.2, 45.8, 49.5, 65.1, 114.3 (d, *J* = 24.4 Hz), 123.1 (d, *J* = 3.1 Hz), 129.6 (d, *J* = 14.7 Hz), 131.3 (d, *J* = 3.7 Hz), 142.5 (d, *J* = 6.6 Hz), 145.0, 146.4, 156.8, 159.6 (d, *J* = 252 Hz), 171.1, 174.9; HRMS (EI) for $C_{22}H_{28}O_4N_6SF$ (MH^+); calcd, 491.1871; found, 491.1870.

cAMP assay:

GPR119 agonists were tested on HEK293S cells over-expressing human GPR119. Changes in cAMP concentrations were assessed using the cAMP dynamic 2 HTRF kit (Cisbio). Cells were diluted in assay buffer (20 mM HEPES pH 7.4, Hank´s Balanced Salt Solution, 0.01 % BSA, 1 mM IBMX) and used at $2x10^3$ cells/well in 384-well plates. Cells were incubated with compound for 45 min before addition of HTRF lysis and detection reagents according to the manufacturer's protocol. Fluorescence readings were captured using an Envision plate reader and cAMP concentrations calculated using a standard curve. The intrinsic activity was expressed as the percent effect compared to that of the control, 50 µM oleoylethanolamide, defined as 100%. A typical standard deviation in $logEC_{50}$ when a compound is

repeated is 0.20 and 0.27 for the human and mouse assays respectively. This translates to 95% of EC_{50} values within 2.5-fold (human) and 3.5-fold (mouse) of a compound's "true" EC_{50}.

Mouse OGTT:

Standard and combination OGTT studies were carried out in-house C57BL6/Jax mice aged 10-11 weeks. GPR119 receptor KO and WT control mice were also bred in house, backcrossed onto a C57BL6/Jax background and used at 10-11 weeks of age.

Overnight (18 hr) fasted mice were dosed via oral gavage (10 mL/kg) with either vehicle (0.1% Pluronic F127), the DPPIV inhibitor sitagliptin, compound **16** or a combination formulation of sitagliptin and compound **16**. At 30 minutes post compound a 2 g/kg oral glucose load (10 mL/kg of 20% glucose in water) was administered. Tail prick blood samples were taken pre-compound (time - 30), pre-glucose (time 0) and at 10, 25, 40, 60 and 90 minutes post glucose load to assess the glucose excursion profile. Glucose levels were measured on a Roche AccuChek hand-held monitor. Improvement in glycaemic control was expressed as percentage reduction in blood glucose AUC normalised to baseline (time 0) glucose levels. This was calculated by comparison to vehicle control using ANCOVA analysis with baseline glucose levels and day of study as covariate factors.

Lean mouse GLP-1:

Mouse GLP-1 levels were assessed in C57BL6/Jax mice at 10-11 weeks of age. Overnight (18 hr) fasted mice were dosed via oral gavage (10 mL/kg) with either vehicle or compound **16**. At 30 minutes post compound administration a terminal blood sample was taken under CO_2/O_2 narcosis *via* cardiac puncture into EDTA blood collection tubes. Plasma was prepared by centrifugation at 13,000 rpm for 5 minutes at 4 °C and frozen at -20 °C until analysis. Samples were analysed for total GLP-1 using the Meso Scale Discovery (MSD) quantitative sandwich chemolumenescent Mouse/Rat ImmunoAssay Kit (Catalogue No. K150FCC). Increase in total GLP-1 compared to vehicle control was assessed by ANOVA analysis of log-transformed data.

Supplementary Material

Complete experimental details for the syntheses of intermediates and all final compounds are described together with crystallographic information. This material is available free of charge via the Internet at http://pubs.acs.org.

Author Information

*Tel: +44 (0)1625 232567. Fax: +44 (0)1625 516667. E-mail: jamie.scott@astrazeneca.com.

Acknowledgements

Alan Birch, Roger Butlin, Sam Groombridge, and Ruth Poultney are thanked for their chemistry contributions. Carina Ämmälä & Laraine Gregory are thanked for their bioscience design contributions and members of the AstraZeneca Animal Science & Welfare group and Dianne Tibbs are thanked both for their work on breeding the mice and their technical support in running the experiments. Johnathan Bright is thanked for statistical analysis of the cAMP assay. Ray Findlay and Seb Degorce are thanked for providing helpful comments on the manuscript.

Abbreviations used

GPR119, G Protein coupled receptor 119; WT, wild-type; KO, knock-out; OEA, oleoylethanolamide; OLDA, *N*-oleoyldopamine; GLP-1, glucagon-like peptide-1; PPB, plasma protein binding; LLE, Ligand-Lipophilicity Efficiency; SAR, structure activity relationship; IA, intrinsic activity; hERG, human ether-a-go-go-related gene; OGTT, oral glucose tolerance test; DPP-IV, Dipeptidyl peptidase-4.

References and Footnotes

1. Fredriksson, R.; Höglund, P. J.; Gloriam, D. E. I.; Lagerström, M. C.; Schiöth, H. B. Seven evolutionarily conserved human rhodopsin G protein-coupled receptors lacking close relatives. *FEBS Lett.* **2003**, *554,* 381-388.

2. Overton, H. A.; Babbs, A. J.; Doel, S. M.; Fyfe, M. C. T.; Gardner, L. S.; Griffin, G.; Jackson, H. C.; Procter, M. J.; Rasamison, C. M.; Tang-Christensen, M.; Widdowson, P. S.; Williams, G. M.; Reynet, C. Deorphanization of a G protein-coupled receptor for oleoylethanolamide and its use in the discovery of small-molecule hypophagic agents. *Cell Metabolism* **2006**, *3,* 167-175.

3. Chu, Z.; Carroll, C.; Chen, R.; Alfonso, J.; Gutierrez, V.; He, H.; Lucman, A.; Xing, C.; Sebring, K.; Zhou, J.; Wagner, B.; Unett, D.; Jones, R. M.; Behan, D. P.; Leonard, J. N-Oleoyldopamine Enhances Glucose Homeostasis through the Activation of GPR119. *Mol. Endocrinol.* **2010**, *24,* 161-170.

4. Chu, Z.; Carroll, C.; Alfonso, J.; Gutierrez, V.; He, H.; Lucman, A.; Pedraza, M.; Mondala, H.; Gao, H.; Bagnol, D.; Chen, R.; Jones, R. M.; Behan, D. P.; Leonard, J. A Role for Intestinal Endocrine Cell-Expressed G Protein-Coupled Receptor 119 in Glycemic Control by Enhancing Glucagon-Like Peptide-1 and Glucose-Dependent Insulinotropic Peptide Release. *Endocrinology* **2008**, *149,* 2038-2047.

5. Chu, Z.; Jones, R. M.; He, H.; Carroll, C.; Gutierrez, V.; Lucman, A.; Moloney, M.; Gao, H.; Mondala, H.; Bagnol, D.; Unett, D.; Liang, Y.; Demarest, K.; Semple, G.; Behan, D. P.; Leonard, J. A Role for β-Cell-Expressed G Protein-Coupled Receptor 119 in Glycemic Control by Enhancing Glucose-Dependent Insulin Release. *Endocrinology* **2007**, *148,* 2601-2609.

6. (a) Fyfe, M. C. T.; McCormack, J. G.; Overton, H. A.; Procter, M. J.; Reynet, C. GPR119 agonists as potential new oral agents for the treatment of type 2 diabetes and obesity. *Expert Opin. Drug Discov.* **2008**, *3,* 403-413; (b) Shah, U. GPR119 agonists: A promising new approach for the treatment of type 2 diabetes and related metabolic disorders. *Current Opinion in Drug Discovery and Development* **2009**, *12,* 519-532; (c) Jones, R. M.; Leonard, J. N.; Buzard, D. J.; Lehmann, J. GPR119 agonists for the treatment of type 2 diabetes. *Expert Opin. Ther. Patents* **2009**, *19,* 1339-1359.

7. (a) Jones, R. M.; Leonard, J. N. Chapter 7 The Emergence of GPR119 Agonists as Anti-Diabetic Agents. In *Annual Reports in Medicinal Chemistry;* John E. Macor, Ed.; Academic Press: 2009; Volume 44, pp 149-170; (b) Shah, U.; Kowalski, T. J. GPR119 Agonists for the Potential Treatment of Type 2 Diabetes and Related Metabolic Disorders. In *Vitamins & Hormones;* Gerald Litwack, Ed.; Academic Press: 2010; Volume 84, pp 415-448; (c) Shah, U.; Edmondson, S.; Szewczyk, J. W. Recent Advances in the Discovery of GPR119 Agonists In *New Therapeutic Strategies for Type 2 Diabetes;* Robert E. Jones, Ed.; RSC Publishing: 2012; Volume 27, pp 177-214.

8. (a) Semple, G.; Fioravanti, B.; Pereira, G.; Calderon, I.; Uy, J.; Choi, K.; Xiong, Y.; Ren, A.; Morgan, M.; Dave, V.; Thomsen, W.; Unett, D. J.; Xing, C.; Bossie, S.; Carroll, C.; Chu, Z.; Grottick, A. J.; Hauser, E. K.; Leonard, J.; Jones, R. M. Discovery of the First Potent and Orally Efficacious Agonist of the Orphan G-Protein Coupled Receptor 119. *J. Med. Chem.* **2008**, *51,* 5172-5175; (b) Semple, G.; Ren, A.; Fioravanti, B.; Pereira, G.; Calderon, I.; Choi, K.; Xiong, Y.; Shin, Y.; Gharbaoui, T.; Sage, C. R.; Morgan, M.; Xing, C.; Chu, Z.; Leonard, J. N.; Grottick, A. J.; Al-Shamma, H.; Liang, Y.; Demarest, K. T.; Jones, R. M. Discovery of fused bicyclic agonists of the orphan G-protein coupled receptor GPR119 with in vivo activity in rodent models of glucose control. *Bioorg. Med. Chem. Lett.* **2011**, *21,* 3134-3141; (c) Semple, G.; Lehmann, J.; Wong, A.; Ren, A.; Bruce, M.; Shin, Y.; Sage, C. R.; Morgan, M.; Chen, W.; Sebring, K.; Chu, Z.; Leonard, J. N.; Al-Shamma, H.; Grottick, A. J.; Du, F.; Liang, Y.; Demarest, K.; Jones, R. M. Discovery of a second generation agonist of the orphan G-protein coupled receptor GPR119 with an improved profile. *Bioorg. Med. Chem. Lett.* **2012**, *22,* 1750-1755.

9. (a) Zhang, J. (K.); Li, A.; Yu, M.; Wang, Y.; Zhu, J.; Kayser, F.; Medina, J. C.; Siegler, K.; Conn, M.; Shan, B.; Grillo, M. P.; Eksterowicz, J.; Coward, P.; Liu, J. (J.) Discovery and optimization of arylsulfonyl 3-(pyridin-2-yloxy)anilines as novel GPR119 agonists. *Bioorg. Med. Chem. Lett.* **2013**, *23,* 3609-3613; (b) Yu, M.; Zhang, J. (K.); Wang, Y.; Zhu, J.; Kayser, F.; Medina, J. C.; Siegler, K.; Conn, M.; Shan, B.; Grillo, M. P.; Coward, P.; Liu, J. (J.) Discovery and optimization of N-(3-(1,3-dioxo-2,3-dihydro-1H-pyrrolo[3,4-c]pyridin-4-yloxy)phenyl)benzenesulfonamides as novel GPR119 agonists.

Bioorg. Med. Chem. Lett. **2014**, *24,* 156-160; (c) Wang, Y.; Yu, M.; Zhu, J.; Zhang, J. (K.); Kayser, F.; Medina, J. C.; Siegler, K.; Conn, M.; Shan, B.; Grillo, M. P.; Liu, J. (J.); Coward, P. Discovery and optimization of 5-(2-((1-(phenylsulfonyl)-1,2,3,4-tetrahydroquinolin-7-yl)oxy)pyridin-4-yl)-1,2,4-oxadiazoles as novel gpr119 agonists. *Bioorg. Med. Chem. Lett.* **2014**, *24,* 1133-1137.

10. (a) Yoshida, S.; Ohishi, T.; Matsui, T.; Tanaka, H.; Oshima, H.; Yonetoku, Y.; Shibasaki, M. Novel GPR119 agonist AS1535907 contributes to first-phase insulin secretion in rat perfused pancreas and diabetic db/db mice. *Biochem. Biophys. Res. Commun.* **2010**, *402,* 280-285; (b) Yoshida, S.; Tanaka, H.; Oshima, H.; Yamazaki, T.; Yonetoku, Y.; Ohishi, T.; Matsui, T.; Shibasaki, M. AS1907417, a novel GPR119 agonist, as an insulinotropic and β-cell preservative agent for the treatment of type 2 diabetes. *Biochem. Biophys. Res. Commun.* **2010**, *400,* 745-751; (c) Yoshida, S.; Ohishi, T.; Matsui, T.; Shibasaki, M. Identification of a novel GPR119 agonist, AS1269574, with in vitro and in vivo glucose-stimulated insulin secretion. *Biochem. Biophys. Res. Commun.* **2010**, *400,* 437-441; (d) Yoshida, S.; Ohishi, T.; Matsui, T.; Tanaka, H.; Oshima, H.; Yonetoku, Y.; Shibasaki, M. The role of small molecule GPR119 agonist, AS1535907, in glucose-stimulated insulin secretion and pancreatic β-cell function. *Diabetes, Obesity and Metabolism* **2011**, *13,* 34-41; (e) Negoro, K.; Yonetoku, Y.; Maruyama, T.; Yoshida, S.; Takeuchi, M.; Ohta, M. Synthesis and structure–activity relationship of 4-amino-2-phenylpyrimidine derivatives as a series of novel GPR119 agonists. *Bioorg. Med. Chem.* **2012**, *20,* 2369-2375; (f) Negoro, K.; Yonetoku, Y.; Misawa-Mukai, H.; Hamaguchi, W.; Maruyama, T.; Yoshida, S.; Takeuchi, M.; Ohta, M. Discovery and biological evaluation of novel 4-amino-2-phenylpyrimidine derivatives as potent and orally active GPR119 agonists. *Bioorg. Med. Chem.* **2012**, *20,* 5235-5246; (g) Negoro, K.; Yonetoku, Y.; Moritomo, A.; Hayakawa, M.; Iikubo, K.; Yoshida, S.; Takeuchi, M.; Ohta, M. Synthesis and structure–activity relationship of fused-pyrimidine derivatives as a series of novel GPR119 agonists. *Bioorg. Med. Chem.* **2012**, *20,* 6442-6451; (h) Oshima, H.; Yoshida, S.; Ohishi, T.; Matsui, T.; Tanaka, H.; Yonetoku, Y.; Shibasaki, M.; Uchiyama, Y. Novel GPR119 agonist AS1669058 potentiates insulin secretion from rat islets and has potent anti-diabetic effects in ICR and diabetic db/db mice. *Life Sci.* **2013**, *92,* 167-173.

11. Wellenzohn, B.; Lessel, U.; Beller, A.; Isambert, T.; Hoenke, C.; Nosse, B. Identification of New Potent GPR119 Agonists by Combining Virtual Screening and Combinatorial Chemistry. *J. Med. Chem.* **2012**, *55,* 11031-11041.

12. (a) Wu, Y.; Kuntz, J. D.; Carpenter, A. J.; Fang, J.; Sauls, H. R.; Gomez, D. J.; Ammala, C.; Xu, Y.; Hart, S.; Tadepalli, S. 2,5-Disubstituted pyridines as potent GPR119 agonists. *Bioorg. Med. Chem. Lett.* **2010**, *20,* 2577-2581; (b) Katamreddy, S. R.; Carpenter, A. J.; Ammala, C. E.; Boros, E. E.; Brashear, R. L.; Briscoe, C. P.; Bullard, S. R.; Caldwell, R. D.; Conlee, C. R.; Croom, D. K.; Hart, S. M.; Heyer, D. O.; Johnson, P. R.; Kashatus, J. A.; Minick, D. J.; Peckham, G. E.; Ross, S. A.; Roller, S. G.; Samano, V. A.; Sauls, H. R.; Tadepalli, S. M.; Thompson, J. B.; Xu, Y.; Way, J. M. Discovery of 6,7-Dihydro-5H-pyrrolo2,3-a]pyrimidines as Orally Available G Protein-Coupled Receptor 119 Agonists. *J. Med. Chem.* **2012**, *55,* 10972-10994.

13. Gillespie, P.; Goodnow Jr., R. A.; Saha, G.; Bose, G.; Moulik, K.; Zwingelstein, C.; Myers, M.; Conde-Knape, K.; Pietranico-Cole, S.; So, S. Discovery of pyrazolo[3,4-d]pyrimidine derivatives as GPR119 agonists. *Bioorg. Med. Chem. Lett.* **2014**, *24,* 949-953.

14. Pham, T. N.; Yang, Z.; Fang, Y.; Luo, J.; Lee, J.; Park, H. Synthesis and biological evaluation of novel 2,4-disubstituted quinazoline analogues as GPR119 agonists. *Bioorg. Med. Chem.* **2013**, *21,* 1349-1356.

15. (a) McClure, K. F.; Darout, E.; Guimarães, C. R. W.; DeNinno, M. P.; Mascitti, V.; Munchhof, M. J.; Robinson, R. P.; Kohrt, J.; Harris, A. R.; Moore, D. E.; Li, B.; Samp, L.; Lefker, B. A.; Futatsugi, K.; Kung, D.; Bonin, P. D.; Cornelius, P.; Wang, R.; Salter, E.; Hornby, S.; Kalgutkar, A. S.; Chen, Y. Activation of the G-Protein-Coupled Receptor 119: A Conformation-Based Hypothesis for Understanding Agonist Response. *J. Med. Chem.* **2011**, *54,* 1948-1952; (b) Mascitti, V.; Stevens, B. D.; Choi, C.; McClure, K. F.; Guimarães, C. R. W.; Farley, K. A.; Munchhof, M. J.; Robinson, R. P.; Futatsugi, K.; Lavergne, S. Y.; Lefker, B. A.; Cornelius, P.; Bonin, P. D.; Kalgutkar, A. S.; Sharma, R.; Chen, Y.

Design and evaluation of a 2-(2,3,6-trifluorophenyl)acetamide derivative as an agonist of the GPR119 receptor. *Bioorg. Med. Chem. Lett.* **2011**, *21,* 1306-1309; (c) Kalgutkar, A. S.; Mascitti, V.; Sharma, R.; Walker, G. W.; Ryder, T.; McDonald, T. S.; Chen, Y.; Preville, C.; Basak, A.; McClure, K. F.; Kohrt, J. T.; Robinson, R. P.; Munchhof, M. J.; Cornelius, P. Intrinsic Electrophilicity of a 4-Substituted-5-cyano-6-(2-methylpyridin-3-yloxy)pyrimidine Derivative: Structural Characterization of Glutathione Conjugates in Vitro. *Chem. Res. Toxicol.* **2011**, *24,* 269-278; (d) Sharma, R.; Eng, H.; Walker, G. S.; Barreiro, G.; Stepan, A. F.; McClure, K. F.; Wolford, A.; Bonin, P. D.; Cornelius, P.; Kalgutkar, A. S. Oxidative Metabolism of a Quinoxaline Derivative by Xanthine Oxidase in Rodent Plasma. *Chem. Res. Toxicol.* **2011**, *24,* 2207–2216; (e). Darout, E.; Robinson, R. P.; McClure, K. F.; Corbett, M.; Li, B.; Shavnya, A.; Andrews, M. P.; Jones, C. S.; Li, Q.,; Minich, M. L.; Mascitti, V.; Guimarães, C. R. W.; Munchhof, M. J.; Bahnck, K. B.; Cai, C.; Price, D. A.; Liras, S.; Bonin, P. D.; Cornelius, P.; Wang, R.; Bagdasarian, V.; Sobota, C. P.; Hornby, S.; Masterson, V. M.; Joseph, R. M.; Kalgutkar, A. S.; Chen, Y. Design and Synthesis of Diazatricyclodecane Agonists of the G-Protein-Coupled Receptor 119. *J. Med. Chem.* **2013**, *56,* 301-319; (f). Futatsugi, K.; Mascitti, V.; Guimarães, C. R. W.; Morishita, N.; Cai, C.; DeNinno, M. P.; Gao, H.; Hamilton, M. D.; Hank, R.; Harris, A. R.; Kung, D. W.; Lavergne, S. Y.; Lefker, B. A.; Lopaze, M. G.; McClure, K. F.; Munchhof, M. J.; Preville, C.; Robinson, R. P.; Wright, S. W.; Bonin, P. D.; Cornelius, P.; Chen, Y.; Kalgutkar, A. S. From partial to full agonism: Identification of a novel 2,4,5,6-tetrahydropyrrolo[3,4-c]pyrazole as a full agonist of the human GPR119 receptor. *Bioorg. Med. Chem. Lett.* **2013**, *23,* 194-197.

16. (a) Xia, Y.; Chackalamannil, S.; Greenlee, W. J.; Jayne, C.; Neustadt, B.; Stamford, A.; Vaccaro, H.; Xu, X.; Baker, H.; O'Neill, K.; Woods, M.; Hawes, B.; Kowalski, T. Discovery of a nortropanol derivative as a potent and orally active GPR119 agonist for type 2 diabetes. *Bioorg. Med. Chem. Lett.* **2011**, *21,* 3290-3296; (b) Szewczyk, J. W.; Acton, J.; Adams, A. D.; Chicchi, G.; Freeman, S.; Howard, A. D.; Huang, Y.; Li, C.; Meinke, P. T.; Mosely, R.; Murphy, E.; Samuel, R.; Santini, C.; Yang, M.; Zhang, Y.; Zhao, K.; Wood, H. B. Design of potent and selective GPR119 agonists for type II diabetes. *Bioorg. Med. Chem. Lett.* **2011**, *21,* 2665-2669.

17 (a). Sakairi, M.; Kogami, M.; Torii, M.; Kataoka, H.; Fujieda, H.; Makino, M.; Kataoka, D.; Okamoto, R.; Miyazawa, T.; Okabe, M.; Inoue, M.; Takahashi, N.; Harada, S.; Watanabe, N. Synthesis and SAR studies of bicyclic amine series GPR119 agonists. *Bioorg. Med. Chem. Lett.* **2012**, *22,* 5123-5128; (b). Sakairi, M.; Kogami, M.; Torii, M.; Makino, M.; Kataoka, D.; Okamoto, R.; Miyazawa, T.; Inoue, M.; Takahashi, N.; Harada, S.; Watanabe, N. Synthesis and Pharmacological Profile of a New Selective G Protein-Coupled Receptor 119 Agonist; 6-((2-Fluoro-3-(1-(3-isopropyl-1,2,4-oxadiazol-5-yl)piperidin-4-yl)propyl)amino)-2,3-dihydro-1*H*-inden-1-one. *Chemical and Pharmaceutical Bulletin* **2012**, *60,* 1093-1095.

18. Zhang, M.; Feng, Y.; Wang, J.; Zhao, J.; Li, T.; He, M.; Yang, D.; Nosjean, O.; Boutin, J.; Renard, P.; Wang, M. High-Throughput Screening for GPR119 Modulators Identifies a Novel Compound with Anti-Diabetic Efficacy in *db/db* Mice. *PLoS ONE* **2013**, *8,* e63861.

19. Sato, K.; Sugimoto, H.; Rikimaru, K.; Imoto, H.; Kamaura, M.; Negoro, N.; Tsujihata, Y.; Miyashita, H.; Odani, T.; Murata, T. Discovery of a novel series of indoline carbamate and indolinylpyrimidine derivatives as potent GPR119 agonists. *Bioorg. Med. Chem.* **2014**, *22,* 1649-1666.

20. (a) Katz, L. B.; Gambale, J. J.; Rothenberg, P. L.; Vanapalli, S. R.; Vaccaro, N.; Xi, L.; Polidori, D. C.; Vets, E.; Sarich, T. C.; Stein, P. P. Pharmacokinetics, Pharmacodynamics, Safety, and Tolerability of JNJ-38431055, a Novel GPR119 Receptor Agonist and Potential Antidiabetes Agent, in Healthy Male Subjects. *Clin. Pharmacol. Ther.* **2011**, *90,* 685-692; (b) Katz, L. B.; Gambale, J. J.; Rothenberg, P. L.; Vanapalli, S. R.; Vaccaro, N.; Xi, L.; Sarich, T. C.; Stein, P. P. Effects of JNJ-38431055, a novel GPR119 receptor agonist, in randomized, double-blind, placebo-controlled studies in subjects with type 2 diabetes. *Diabetes, Obesity and Metabolism* **2012**, *14(8)*, 709-716.

21. Polli, J. W.; Hussey, E.; Bush, M.; Generaux, G.; Smith, G.; Collins, D.; McMullen, S.; Turner, N.; Nunez, D. J. Evaluation of drug interactions of GSK1292263 (a GPR119 agonist) with statins: from in vitro data to clinical study design. *Xenobiotica* **2013**, *43,* 498-508.

22. (a) Brocklehurst, K. J.; Broo, A.; Butlin, R. J.; Brown, H. S.; Clarke, D. S.; Davidsson, Ö.; Goldberg, K.; Groombridge, S. D.; Kelly, E. E.; Leach, A.; McKerrecher, D.; O'Donnell, C.; Poucher, S.; Schofield, P.; Scott, J. S.; Teague, J.; Westgate, L.; Wood, M. J. M. Discovery, optimisation and in vivo evaluation of novel GPR119 agonists. *Bioorg. Med. Chem. Lett.* **2011**, *21,* 7310-7316; (b) Scott, J. S.; Birch, A. M.; Brocklehurst, K. J.; Broo, A.; Brown, H. S.; Butlin, R. J.; Clarke, D. S.; Davidsson, Ö.; Ertan, A.; Goldberg, K.; Groombridge, S. D.; Hudson, J. A.; Laber, D.; Leach, A. G.; MacFaul, P. A.; McKerrecher, D.; Pickup, A.; Schofield, P.; Svensson, P. H.; Sörme, P.; Teague, J. Use of Small-Molecule Crystal Structures To Address Solubility in a Novel Series of G Protein Coupled Receptor 119 Agonists: Optimization of a Lead and in Vivo Evaluation. *J. Med. Chem.* **2012**, *55,* 5361-5379; (c) Scott, J. S.; Birch, A. M.; Brocklehurst, K. J.; Brown, H. S.; Goldberg, K.; Groombridge, S. D.; Hudson, J. A.; Leach, A. G.; MacFaul, P. A.; McKerrecher, D.; Poultney, R.; Schofield, P.; Svensson, P. H. Optimisation of aqueous solubility in a series of G protein coupled receptor 119 (GPR119) agonists. *Med. Chem. Commun.* **2013**, *4,* 95-100; (d) Scott, J. S.; Brocklehurst, K. J.; Brown, H. S.; Clarke, D. S.; Coe, H.; Groombridge, S. D.; Laber, D.; MacFaul, P. A.; McKerrecher, D.; Schofield, P. Conformational restriction in a series of GPR119 agonists: Differences in pharmacology between mouse and human. *Bioorg. Med. Chem. Lett.* **2013**, *23,* 3175-3179.

23. Easter, A.; Sharp, T. H.; Valentin, J.-P.; Pollard, C. E. Pharmacological validation of a semi-automated in vitro hippocampal brain slice assay for assessment of seizure liability. *J. Pharmacol. Toxicol. Methods* **2007**, *56,* 223-233.

24. The intrinsic activity was expressed as the percent effect compared to that of the control, 50 μM oleoylethanolamide, defined as 100% as per; Ariens, E. J. Affinity and intrinsic activity in the theory of competitive inhibition. I. Problems and theory. *Arch. Int. Pharmacodyn. Ther.* **1954**, *99*, 32-49.

25. hERG measurements were made as described in; Bridgland-Taylor, M. H.; Hargreaves, A. C.; Easter, A.; Orme, A.; Henthorn, D. C.; Ding, M.; Davis, A. M.; Small, B. G.; Heapy, C. G.; Abi-Gerges, N.; Persson, F.; Jacobson, I.; Sullivan, M.; Albertson, N.; Hammond, T. G.; Sullivan, E.; Valentin, J. -P.;

Pollard, C. E. Optimisation and validation of a medium-throughput electrophysiology-based hERG assay using IonWorks™ HT. *J. Pharmacol. Toxicol. Methods* **2006**, *54,* 189-199.

26. The small decrease in lipophilicity associated with the transformation $ArSO_2Me$ to $ArCH_2SO_2Me$ ($\Delta logD_{7.4}$ -0.2) was exactly as predicted by clogP (-0.2). In the AstraZeneca compound collection we found ten other matched pair examples with measured $logD_{7.4}$ data with this change and all showed a decrease in lipophilicity (mean $\Delta logD_{7.4}$ = -0.2; range = -0.1 to -0.6)

27. $logD_{7.4}$, plasma-protein binding and solubility measurements were made as described in; Buttar, D.; Colclough, N.; Gerhardt, S.; MacFaul, P. A.; Phillips, S. D.; Plowright, A.; Whittamore, P.; Tam, K.; Maskos, K.; Steinbacher, S.; Steuber, H. A. Combined spectroscopic and crystallographic approach to probing drug–human serum albumin interactions. *Bioorg. Med. Chem.* **2010**, *18,* 7486-7496.

28. The increase in lipophilicity observed when replacing a CH_2 with a O ($\Delta logD_{7.4}$ +0.8) may seem counterintuitive, but it is predicted by clogP (+1.1) in the case of an $arylCH_2sulfone$. Five other molecular matched pairs with this transform and measured $logD_{7.4}$ data were found in the AstraZeneca collection and all showed an increase in lipophilicity (mean $\Delta logD_{7.4}$ = +0.8; range = +0.4 to +1.0)

29. Ertan, A.; Goldberg, K.; Groombridge, S.; Hudson, J.; Leach, A. G.; Pickup, A.; Poultney, R.; Scott, J. S.; Svensson, P. H.; Sweeney, J.; MacFaul, P. A. Oxadiazole isomers: all bioisosteres are not created equal. *Med. Chem. Commun.* **2012**, *3*, 600-604.

30. Figure 3A contains 162 compounds made within the project with the substructure **A**. For the matched pair analysis of the oxadiazoles substructures **B** (1,3,4) and **C** (1,2,4) were used.

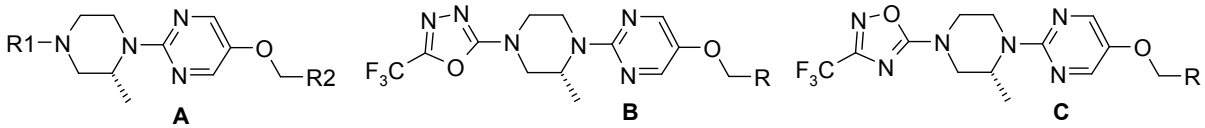

31. The media contained an aqueous mixture of TRIZMA (tris(hydroxymethyl)aminomethane) maleate, taurocholic acid, phosphatidyl choline, oleic acid, 1-oleoyl-rac-glycerol, sodium chloride at pH 6.4 and corresponds to media 2 in; Lue, B.-M.; Flemming, S. N.; Magnussen, T.; Schou, H. M.; Kristensen, K.; Jacobsen, L. O.; Müllertz, A. *Eur. J. Pharm. Biopharm.,* **2008***, 69,* 648-657. The solubility figure quoted here was measured after one hour and did not changed significantly over a 24 hour period.

32. The degredation product was identified as the piperazine, corresponding to loss of the trifluoro-oxadiazole group, with a predicted degredation half-life of 2.5 days at 25 ^{o}C.

33. All *in vivo* studies were randomised, blocked across test days when a study had to be run over two days and were designed to have 80% power to detect effects of the desired size. A positive control was used to monitor the reproducibility of models. GLP-1 data was log transformed. ANOVA with contrasts was used where appropriate to compare groups of interest. ANCOVA with contrasts was used where necessary to adjust for the covariates baseline levels (for glucose) or day effects when a study was split over two days. Where LSmeans are shown, this indicates that ANCOVA has been used. Significance is denoted as follows: * $p < 0.05$, ** $p < 0.01$, *** $p < 0.001$.

34. (a) Deacon, C. F. Dipeptidyl peptidase-4 inhibitors in the treatment of type 2 diabetes: a comparative review. *Diabetes, Obesity and Metabolism* **2011**, *13,* 7-18; (b) Marketed Small Molecule Dipeptidyl Peptidase IV (DPP4) Inhibitors as a New Class of Oral Anti-Diabetics In *New Therapeutic Strategies for Type 2 Diabetes;* Robert E. Jones, Ed.; RSC Publishing: 2012; Vol. Volume 27, pp 15-28.

Table of Contents Graphic

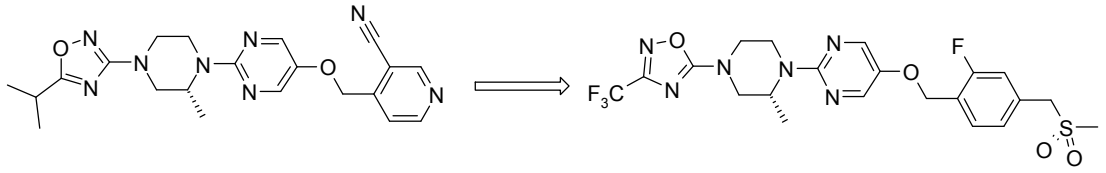

1		**16**	
GPR119 EC_{50}	8 nM (269%)	GPR119 EC_{50}	11 nM (84%)
hERG IC_{50}	10 μM	hERG IC_{50}	>30 μM
$LogD_{7.4}$	3.3	$LogD_{7.4}$	3.6
Brain Slice Assay	positive signal	Brain Slice Assay	no signal observed